

**Expression and properties of  
neuronal MHC class I molecules  
in the brain of the common marmoset monkey**

**PhD Thesis**

in partial fulfillment of the requirements  
for the degree “Doctor rerum naturalium”  
in the Molecular Biology Program  
at the Georg August University Göttingen,  
Faculty of Biology

**submitted by**

Adema Ribic

**born in**

Jajce, Bosnia and Herzegovina

**2009**

**Declaration**

I hereby declare that this submission is my own work and that, to the best of my knowledge and belief, it contains no materials previously published or written by another person nor material which to a substantial extent has been accepted for the award of any other degree of the university or other institute of higher education, except where due acknowledgment has been made in the text.

**Signature**

**Name**

**Date and place**

.....

.....

.....

## List of publications

Ribic A, Flügge G, Schlumbohm C, Mätz-Rensing K, Walter L, Fuchs E: Activity-dependent regulation of MHC class I expression in the developing primary visual cortex of marmoset monkeys, *submitted to Neuroscience*

Ribic A, Zhang M, Schlumbohm C, Mätz-Rensing K, Uchanska-Ziegler B, Flügge G, Zhang W, Walter L, Fuchs E: Neuronal MHC class I molecules are involved in excitatory synaptic transmission at the hippocampal mossy fiber synapses of marmoset monkeys, *under review, J Neuroscience*

Abumaria N, Ribic A, Anacker C, Fuchs E, Flügge G (2008) Stress upregulates TPH1 but not TPH2 mRNA in the dorsal raphe nucleus: Identification of two TPH2 mRNA splice variants. *Cell Mol Neurobiol* 28: 331-342

## **Table of contents**

<b>Acknowledgements</b>	<b>8</b>
<b>Abstract</b>	<b>10</b>
<b>List of tables and figures</b>	<b>12</b>
<b>Abbreviations</b>	<b>14</b>
<b>1. Introduction</b>	<b>16</b>
1.1. The major histocompatibility complex	16
1.2. Major histocompatibility complex class I	17
1.3. MHC class I signaling in immune and non-immune systems	19
1.4. Immune privilege and neuronal expression of MHC class I molecules	21
1.5. MHC class I molecules in the visual system	22
1.6. MHC class I molecules in the hippocampus	25
1.7. The common marmoset as a model system	26
1.8. Aims of the study	28
<b>2. Materials and methods</b>	<b>29</b>

<b>2.1. Animals</b>	<b>29</b>
<b>2.2. Brain sections</b>	<b>30</b>
<b>2.3. PCR cloning of MHC class I transcripts</b>	<b>31</b>
<b>2.4. In situ hybridization</b>	<b>31</b>
<b>2.5. Quantitative in situ hybridization</b>	<b>32</b>
<b>2.6. Quantitative RT-PCR</b>	<b>33</b>
<b>2.7. Immunocytochemistry for light microscopy</b>	<b>34</b>
<b>2.8. Immunofluorescence and confocal microscopy</b>	<b>37</b>
<b>2.9. Protein extraction</b>	<b>39</b>
<b>2.10. Antibody purification and dialysis</b>	<b>40</b>
<b>2.11. Immunoblot analysis</b>	<b>40</b>
<b>2.12. Image analysis of sections from monocularly enucleated animals</b>	<b>41</b>
<b>2.13. Cell culture, immunoprecipitation and protein purification</b>	<b>41</b>
<b>2.14. Electrophysiology</b>	<b>42</b>
<b>3. Results</b>	<b>45</b>
<b>3.1. Part I: MHC class I molecules in the visual cortex</b>	<b>45</b>
3.1.1. Expression of MHCI in the visual system of the common marmoset	45

3.1.2. MHC class I expression levels are regulated by neuronal activity	53
3.1.3. Neurons expressing higher levels of MHC class I are innervated by afferents from the intact eye	55
<b>3.2. Part II: the hippocampus</b>	<b>59</b>
3.2.1. Expression of MHC class I molecules in the hippocampus of the common marmoset	59
3.2.2. A subset of MHC class I proteins is localized on the presynaptic side of the mossy fiber-CA3 synapse	63
3.2.3. MHC class I proteins are present on the giant mossy fiber terminals	64
3.2.4. Neuronal MHC class I proteins are involved in excitatory transmission at mossy-fiber CA3 synapses in the marmoset hippocampus	66
<b>4. Discussion</b>	<b>69</b>
<b>4.1. Cellular localization of MHC class I molecules in the visual cortex</b>	<b>69</b>
<b>4.2. MHC class I in the developing visual system</b>	<b>70</b>
<b>4.3. MHC class I expression in the visual cortex is activity dependent</b>	<b>71</b>
<b>4.4. Localization of MHC class I molecules in the hippocampus</b>	<b>74</b>
<b>4.5. MHC class I involvement in excitatory transmission at the mossy fiber-CA3 synapse</b>	<b>76</b>
4.5.1. Implications of antibody application in electrophysiological recordings	76

4.5.2. Potential function of MHC class I molecules in synaptic transmission at the mossy fiber-CA3 synapse	78
<b>Summary and conclusions</b>	<b>81</b>
<b>References</b>	<b>83</b>
<b>Curriculum Vitae</b>	<b>92</b>

## Acknowledgements

First spots in thesis acknowledgements usually belong to thesis supervisor(s); however, as a student from the waiting list for the admission to the MolBio program, I have to make an exception since I am most indebted to Dr. Steffen Burkardt and the MolBio Coordination office for me being here and for the great job they have done concerning all student issues throughout the past years. I also have another program to thank for funding a very large part of my project and me, the NEUREST and its team: Dr. Joachim Bormann and paperwork-happy Eva Strehler and Dr. Thomas Fritsche.

I am grateful to my MolBio supervisor, Dr. Lutz Walter, for giving me a chance to work on this project and for allowing me to work as independently as I could, with full support from his side. Kudos also go to the people in his lab, especially to my fellow nicotine addict Philip, who made those brief mental breaks less dull.

I am more than thankful to my NEUREST supervisor, Prof. Eberhard Fuchs, who provided space for me in his lab although I was a relatively unplanned addition to the lab personnel. Furthermore, I would like to thank him for having time for me whenever I needed guidance and most of all for trusting me with things almost everyone deemed either too difficult or impossible to do. Luckily, it turned out that “difficult takes a day, and impossible takes a week”. Special thanks goes to Prof. Gabriele Flügge, for all the support and advice she provided throughout these past three years.

Start of the thesis can get a bit tough on anyone, so I am particularly thankful to the past members of the Clinical Neurobiology Lab for providing tips and tricks necessary for survival: Nash and Ben for giving me a warm welcome and company in otherwise turmoil beginner times, and Anna for keeping me company in the lab void and most of all for being responsible for my not so bad state of German language skills today. I am additionally grateful to Ben, who provided significant amount of help and advice when it came to work. Big thanks also goes out to Christina, Kerstin and especially to Julia and Cornelia for all the help with the animals, as well as to Andreas for all the tech support. Nicole, Carolina and Kerstin-thank you for bringing life, sounds and piles of chocolate to the B1.05 with you (the chocolate is especially appreciated).

One of the vital experiments of my thesis would not have been possible to perform without Prof. Weiqi Zhang, who generously provided me with his lab and all of its assets for

almost a year. I would like to thank Lucian, for help with setting things up and especially to Mingyue, for displaying enormous amount of patience needed to work through electrophysiology experiments with a fidgety molecular biologist.

Moreover, I am indebted to my thesis committee members, Prof. Nils Brose and Prof. Jürgen Wienands, whose support and ideas made them a thesis committee a PhD student can only wish and hope for.

The past three years would have been far harder to live through if there weren't for people that kept me company outside of the lab-or to put it better, who managed to put up with me all this time: my homie Konstantina, and the designated driver of severely sunburned, barely walking people, Kathy. Most of all, the company of the support group members will never be forgotten: my flatmate Mare, for long-lasting company and unforgettable wingwomanship; Achim, for keeping my wit defenses at a level necessary for surviving vacations at home, and Andrew, for most ingenious presents and for being a rock-steady bud all this time.

Lastly, but most importantly, I would like to thank my family, both indigenous and extended members, for all the love that has managed to keep me relatively sane, safe and sound. This thank you specially extends to my dad, who although long gone, still feels as if he never left.

Finally, I dedicate this to my own personal Lights of Eärendil, my mom, my sister and my niece Asja, who gave me the world in a grain of sand.

## Abstract

Several recent studies have highlighted the important role of immunity-related molecules in synaptic plasticity processes in the developing and adult rodent brain. It has been suggested that neuronal MHC (major histocompatibility complex) class I genes play a role in the refinement and pruning of synapses in the developing visual system and in certain forms of plasticity in the hippocampus. The aim of this study was to investigate the expression pattern and levels of MHC class I (MHCI) molecules throughout the development of the visual system and the hippocampus in a nonhuman primate, the common marmoset (*Callithrix jacchus*).

The first part of this thesis describes expression of MHCI molecules in the visual cortex of the common marmoset monkey. Analysis of the neurons of the marmoset visual cortex revealed high levels of expression of MHCI genes very early in postnatal development, at a stage when synaptogenesis takes place and ocular dominance columns are formed. To determine whether MHC class I gene expression levels are regulated by retinal activity, animals were subjected to monocular enucleation, which is a method known to induce an ocular dominance shift in the visual cortex. MHC class I mRNA expression was higher in response to monocular enucleation. Furthermore, MHC class I immunoreactivity revealed variations in staining intensity of layer IV neurons in the visual cortex of enucleated animals, which was not observed in control animals. The pattern of MHC class I immunoreactivity indicated that higher expression levels were associated with retinal activity coming from the intact eye. These observations demonstrate that, in the primate brain, neuronal MHC class I gene expression is regulated by neuronal activity. Moreover, they extend previous findings

by suggesting a role for neuronal MHC class I molecules during synaptogenesis in the visual cortex.

The second part of the thesis describes expression of MHCI molecules in the hippocampal formation. MHCI mRNA is present at high levels in all subregions of the hippocampus (in dentate gyrus, hilus and areas CA1-CA3). However, a presynaptic, mossy-fiber-specific localization of MHCI proteins within the marmoset hippocampus was observed. MHCI molecules are present in the large VGlut1-positive mossy-fiber terminals, which provide input to CA3 pyramidal neurons. Furthermore, whole-cell recordings of CA3 pyramidal neurons in acute hippocampal slices of the common marmoset demonstrated that application of antibodies which specifically block MHCI proteins caused a significant decrease in the frequency and a transient increase in the amplitude of sEPSCs (spontaneous excitatory postsynaptic currents) in CA3 pyramidal neurons. These findings allude to a role of MHCI molecules in plasticity processes at the primate mossy fiber-CA3 synapses.

Taken together, the present thesis describes in detail expression of MHCI molecules in the common marmoset visual system and the hippocampus. Furthermore, it extends previous studies in other model animals by implicating neuronal MHCI in synaptogenesis in the visual cortex and in the plasticity of the hippocampal mossy fiber synapses.

## List of tables and figures

### Tables

<b>Table 1.</b> List of antibodies used for detection of neuronal, glial and synaptic markers and the dilutions used	<b>39</b>
--	-----------

### Figures

<b>Figure 1.</b> Structure of MHC class I molecules	<b>17</b>
<b>Figure 2.</b> T-cell receptor signaling	<b>20</b>
<b>Figure 3.</b> Structure of the mammalian visual system	<b>23</b>
<b>Figure 4.</b> Effects of monocular deprivation on visual cortex development	<b>24</b>
<b>Figure 5.</b> Schematic structure of the hippocampus	<b>25</b>
<b>Figure 6.</b> Schematic representation of recording chamber setup	<b>44</b>
<b>Figure 7.</b> Lack of MHC class I expression in the lateral geniculate nucleus as revealed by <i>in situ</i> hybridization	<b>45</b>
<b>Figure 8.</b> Expression of MHC class I in the visual cortex as revealed by <i>in situ</i> hybridization	<b>46</b>
<b>Figure 9.</b> MHC class I protein levels follow synaptogenesis	<b>48</b>
<b>Figure 10.</b> MHC class I immunoreactivity in the visual cortex of the common marmoset	<b>49</b>
<b>Figure 11.</b> MHC class I protein colocalizes with the neuronal marker MAP2 in layer IV neurons of the visual cortex	<b>49</b>
<b>Figure 12.</b> MHC class I protein is localized to both inhibitory and excitatory neurons in the visual cortex	<b>51</b>
<b>Figure 13.</b> MHC class I protein is localized on radial glial cells in occipital lobes	<b>52</b>
<b>Figure 14.</b> MHC class I mRNA expression levels are upregulated in response to monocular enucleation	<b>54</b>

<b>Figure 15.</b> Quantitative <i>in situ</i> hybridization of MHC class I mRNA	<b>54</b>
<b>Figure 16.</b> Layer IV of visual cortex reveals a banded pattern of MHC class I and c-Fos immunoreactivity in enucleated animals	<b>57</b>
<b>Figure 17.</b> Neurons exhibiting higher MHC class I levels are receiving afferents from the intact eye	<b>58</b>
<b>Figure 18.</b> MHC class I genes are strongly expressed in the marmoset hippocampus	<b>60</b>
<b>Figure 19.</b> MHC class I protein is expressed in the mossy fiber pathway	<b>62</b>
<b>Figure 20.</b> MHC class I protein is localized on the presynaptic side of the mossy fiber-CA3 synapse	<b>64</b>
<b>Figure 21.</b> MHC class I protein is present on large mossy fiber boutons	<b>65</b>
<b>Figure 22.</b> HCA2 and HC10 recognize native marmoset MHC class I protein	<b>66</b>
<b>Figure 23.</b> Application of antibodies against MHC class I proteins to marmoset hippocampal slices decreases frequency of sESPCs	<b>68</b>
<b>Figure 24.</b> Schematic representation of effects of monocular deprivation	<b>72</b>
<b>Figure 25.</b> Schematic representation of potential mode of action of MHC class I at the mossy fiber-CA3 synapse	<b>79</b>

## **Abbreviations**

CA1 Cornu Ammonis 1

CA3 Cornu Ammonis 3

CNS central nervous system

CO cytochrome oxidase

GFAP glial fibrillary acidic protein

LGN lateral geniculate nucleus

LTD long term depression

LTP long term potentiation

MAP2 microtubule associated protein 2

ME monocular enucleation

mEPSCs miniature excitatory postsynaptic currents

MHC major histocompatibility complex

MHCI major histocompatibility complex class I

ODC ocular dominance column

qRT-PCR quantitative real time polymerase chain reaction

RT room temperature

SAP102 synapse associated protein of 102 kDa

SDS-PAGE sodium-dodecyl-sulphate polyacrylamide gel electrophoresis

sEPSCs spontaneous excitatory postsynaptic currents

SNAP-25 synaptosome-associated protein of 25 kDa

Sv2b synaptic vesicle protein 2b

synCAM synaptic cell adhesion molecule

V1 primary visual cortex

VGlut1 vesicular glutamate transporter 1

VGlut2 vesicular glutamate transporter 2

# 1. Introduction

## 1.1. The major histocompatibility complex

The major histocompatibility complex (MHC) is a dense cluster of genes found in all jawed vertebrates (Kelley et al., 2005). The majority of genes encoded by the MHC cluster are involved in immune responses, mainly in antigen presentation. The MHC family is generally divided into three classes: I, II and III (Kelley et al., 2005). Genes of all three classes encode proteins involved in both immune and non-immune processes; however, class I and II MHC molecules are the most investigated members of this large family due to their essential role in antigen presentation. Both class I and class II MHC genes are extremely polymorphic and encode transmembrane glycoproteins responsible for presentation of antigenic peptides to T lymphocytes. They differ, however, in their general properties, roles and structure. MHC class I (MHC I) molecules are ubiquitously expressed and involved in immune surveillance and presentation of “endogenous peptides” to cytotoxic T lymphocytes (Kaufman et al., 1994). Endogenous peptides are usually 9-15 amino acids long and are derived from proteolytic processing of intracellular pathogens (“non-self” antigens), as well as from diverse cellular proteins that usually end their cycle in the proteasome (“self” antigens). Expression of MHC class II molecules is mainly confined to specialized antigen presenting cells (APCs), such as macrophages, dendritic cells and B lymphocytes (Kaufman et al., 1994). They present “exogenous peptides” derived from extracellular pathogens to helper T cells.

## 1.2. Major histocompatibility complex class I

Major histocompatibility class I (MHCI) molecules are found on virtually all nucleated cells in the body and are the most polymorphic molecules described to date (Solheim, 1999; Cresswell et al., 2005). They are composed of three subunits: a transmembrane heavy chain, a small  $\beta$ -2-microglobulin subunit and the presenting peptide (Figure 1, A and B, Solheim, 1999; Cresswell et al., 2005).

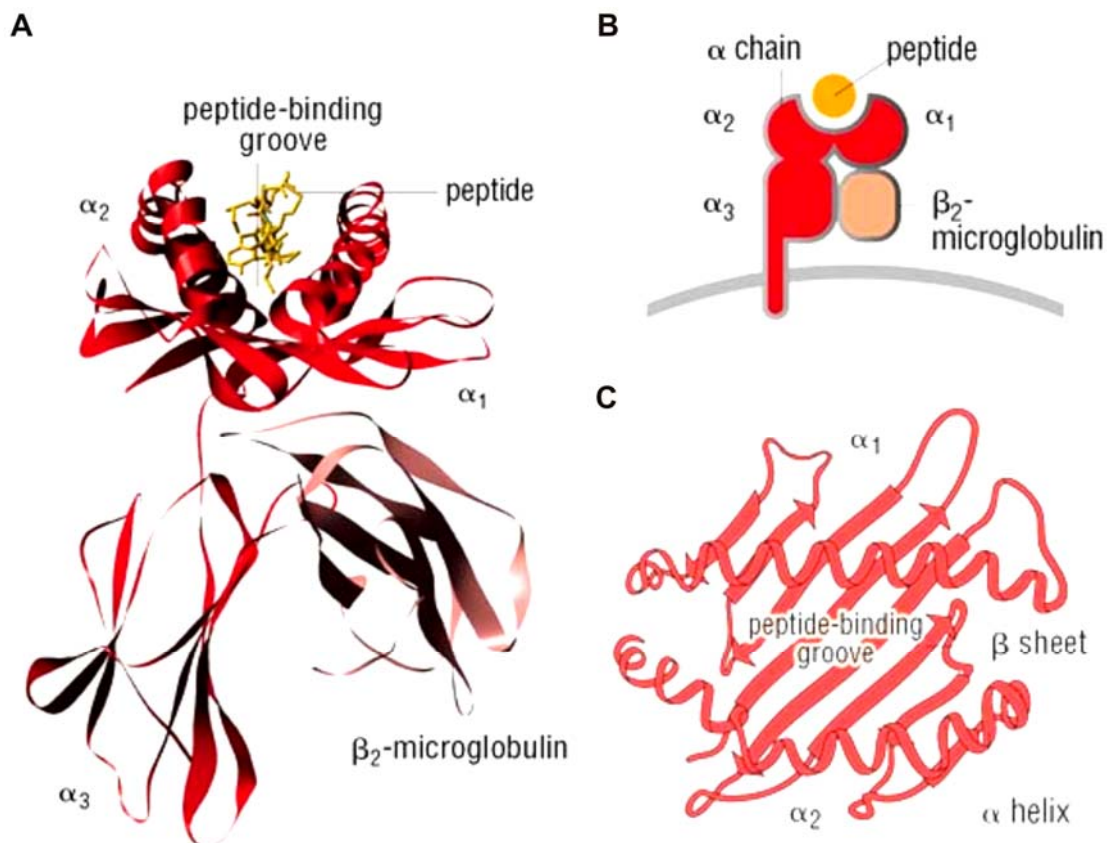


**Figure 1. Structure of MHC class I molecules.** (A) Ribbon structure of MHC class I (MHCI) molecule: MHCI molecule is composed of heavy chain (red),  $\beta$ -2-microglobulin (brown) and the presenting peptide (yellow). Immunoglobulin fold structure of the  $\alpha_3$  domain of the heavy chain and the  $\beta$ -2-microglobulin is visible. (B) Schematic representation of MHCI structure. (C) Structure of MHCI peptide binding groove formed by  $\alpha_1$  and  $\alpha_2$  helices. Modified from "Immunity: The Immune Response in Infectious and Inflammatory Disease", OUP Oxford, 2007.

MHCI molecules are assembled in the endoplasmatic reticulum with the help of chaperons and are usually dependent on the presence of all three subunits for reaching the cell surface. The MHCI heavy chain is a glycoprotein with reported molecular weight of 42-48 kDa and consists of three extracellular domains ( $\alpha$ 1-3), and short transmembrane and cytoplasmic regions.  $\alpha$ 1 and  $\alpha$ 2 domains form the peptide binding groove and are the regions responsible for the high polymorphism of MHCI molecules (Figure 1, A and C).  $\alpha$ 3 domain carries the signature of the immunoglobulin superfamily, the immunoglobulin fold.  $\beta$ -2-microglobulin is the smaller subunit of 11-13 kDa. It is without a transmembrane domain and it is non-covalently attached to the MHCI heavy chain on the cell surface.  $\beta$ -2-microglobulin is encoded by a gene settled outside of the MHC cluster and it is structurally also immunoglobulin-like (Figure 1, A). MHCI molecules are divided in two groups: classical and non-classical MHCI. Classical MHCI molecules are polymorphic, usually present as trimers on the cells surface and are mainly associated with antigen presentation. Non-classical MHCI molecules are still somewhat of an enigma. They are not as polymorphic as the classical MHCI and some of them do not require  $\beta$ -2-microglobulin or the binding of peptide in order to reach the cell surface. Non-classical MHCI are also implicated in a wide range of immune and non-immune processes, from presentation of glycolipids, instead of peptides, to regulation of pheromone signaling (Arosa et al., 2007).

As previously mentioned, MHC molecules are present in all jawed vertebrates (Kelley et al., 2005). The number of class I genes is highly variable between species; moreover, orthologous relationships are found only within same order of mammals such as within primates, but never between primates and rodents (Kumanovics et al., 2003; Günther and Walter, 2001). Mouse and rat MHC clusters are designated as H2 and RT1 respectively and both are comprised of over 30 functional classical and non-classical genes (Ioannidu et al.

2001; Kumanovics et al., 2003). Even among different inbred strains of rats or mice, the number of MHC I genes is variable (Kulski et al., 2002; Roos and Walter, 2005). The human MHC cluster, also known as HLA (human leukocyte antigen) complex, contains six functional classical human MHC I genes (Kelley et al. 2005). Despite the orthologous relationship, MHC I genes are still very variable between primates. Strict HLA orthologues of classical HLA class genes HLA-A, -B, or -C are present only in great apes, whereas orthologues of the non-classical HLA-E and HLA-F genes are found in Old World (baboons, macaques) and New World monkeys. The MHC of New World monkeys is poorly characterized due to lack of available genome sequences. In marmoset monkeys (*Callithrix jacchus*) only two MHC genes have been characterized, Caja-G and Caja-E (Cadavid et al., 1998), which represent classical and non-classical class I genes, respectively.

### **1.3. MHC class I signaling in immune and non-immune systems**

Cytotoxic T-cells become activated through the T-cell receptor complex (TCR) after they recognize the MHC I-presented peptide as foreign and potentially hazardous. Affinity of TCR for the MHC I complex on the cell surface becomes strong if a peptide is a “non-self” peptide. The TCR is composed of the main TCR  $\alpha$  and  $\beta$  chains and CD3 subunits ( $\gamma$ ,  $\delta$ ,  $\epsilon$  and  $\zeta$ , Figure 2, A) that bear a number of immunoreceptor tyrosine based activatory motifs (ITAMs). CD8 and CD4 are co-receptors involved in recognition of MHC I and class II molecules, respectively. After TCR contacts the MHC I, CD8 co-receptor and TCR-associated kinase Lck are brought closer within the membrane to the CD3 subunits (Figure 2, B). The proximity of Lck kinase to TCR enables it to phosphorylate ITAMs located in the

TCR (Figure 2, B). Phosphorylated ITAMs are then able to recruit cytoplasmic kinase ZAP-70 which then in turn phosphorylates an adaptor protein, LAT (linker of T-cell activation). This sets in motion a cascade that leads to cytoskeletal rearrangements and cytokine production; in other words, T-cell becomes activated. Although this is the canonical MHC I signaling pathway, the TCR complex is not the only receptor for the MHC I molecules. MHC I are able to interact with a large number of receptors within the immune system, both in *cis* and in *trans*, such as killer-cell immunoglobulin-like receptors (KIRs), leukocyte immunoglobulin-like receptors (LILRs), etc., causing a wide range of responses (Parham, 2005).

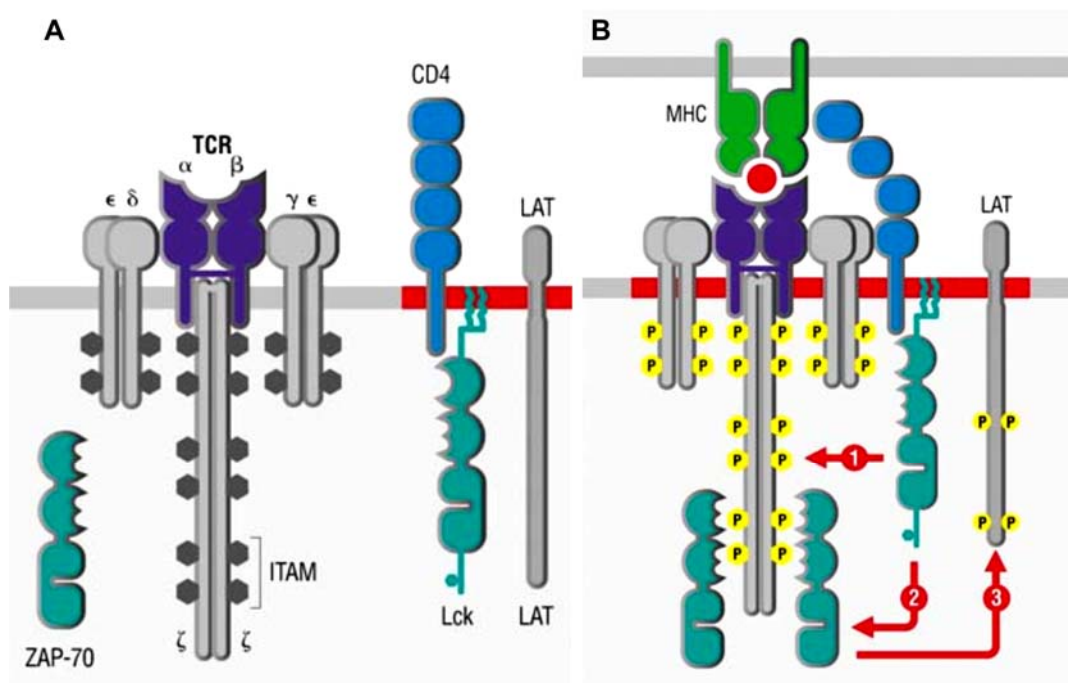


**Figure 2. T-cell receptor signaling.** (A) Schematic structure of T-cell receptor complex (TCR). (B) Steps of signaling cascade initiated after TCR recognizes the peptide presented by MHC I as foreign: 1. TCR subunit rearrangement within the cell membrane; 2. Lck phosphorylates ITAMs within the CD3 and ZAP-70; 3. ZAP-70 phosphorylates LAT which precedes T-cell activation. Modified from "Immunity: The Immune Response in Infectious and Inflammatory Disease", OUP Oxford, 2007.

Outside of the immune system, MHC I have been implicated mainly in the regulation of trafficking and internalization of hormone receptors. Interactions with the insulin receptor (IR), the  $\gamma$ -endorphin receptor, the luteinizing hormone receptor and many others have been reported (Arosa et al., 2007). The best characterized non-immune interaction of MHC I is with the insulin receptor. It has been suggested that MHC I are involved in the glycosylation of IR and its transport to the cell surface, but most evidence has been provided for the role of MHC I in IR internalization. A number of studies have suggested that MHC I associates with IR after insulin binding thereby causing its internalization and removal from the cell surface. Functional significance of these findings is still debated; however, certain MHC I genes have been implicated in the etiology of type I diabetes (Fernando et al., 2008).

#### **1.4. Immune privilege and neuronal expression of MHC class I molecules**

The concept of immune privilege refers to the ability of certain organs (eyes, brain, testicles and the uterus while harboring a fetus) to evade inflammatory responses during antigen presentation (Hong and Van Kaer, 1999). A classical inflammatory response would be devastating for immune privileged structures due to their special properties and it is believed that immune privilege is an active process that has developed throughout evolution (Hong and Van Kaer, 1999). The central nervous system (CNS) is an immune privileged site and as such has long been considered devoid of neuronal MHC I expression. Based on experimental evidence, it was believed that neurons were able to express MHC I only after induction by cytokines (Neumann et al., 1995). However, a study in 1998 (Corriveau et al.) demonstrated high neuronal MHC I expression in normal, non-injured brains. Since then, a

number of studies confirmed that neurons do express MHC I molecules in normal conditions (Huh et al., 2000; Rölleke et al., 2006; Goddard et al., 2007; McConnell et al., 2009). Furthermore, MHC I have been implicated in proper development and maintenance of neuronal circuitry in various brain regions, especially in the development of the visual system, and in the modulation of synaptic plasticity in hippocampus and the cerebellum (Huh et al., 2000; Goddard et al., 2007; McConnell et al., 2009).

### **1.5. MHC class I molecules in the visual system**

Synaptic plasticity is the ability of neurons to change the strength of their synaptic connections in response to various stimuli. This process occurs in various forms with distinct properties and is thought to be fundamental for development and maintenance of brain circuits. The developing visual system is one of the main models of two forms of plasticity: visual activity-independent and visual input-driven or activity-dependent plasticity. There are two main stages of visual system development. The early stage encompasses the development of the eyes and the brain and the initial development of the neuronal connections between them. It is believed that at this early stage, both growth of neuronal processes and pathfinding are independent of retinal activity, as opposed to the later stage. The second stage involves proper development of connections in and between the thalamus and the visual cortex, both of which are regions responsible for the processing of the visual input. The thalamic dorsal lateral geniculate nucleus (LGN) is the first relay structure of visual input and is organized into segregated, eye-specific, neuronal layers that form upon early spontaneous activity from retinal ganglion cells in the eye (Figure 3, Shatz, 1996).

Neurons of the LGN send their projections to the primary visual cortex (V1), where their activity is required for the development of eye-specific patches of neurons in layer IV, i.e., the ocular dominance columns (ODCs) (Sur et al., 2005).

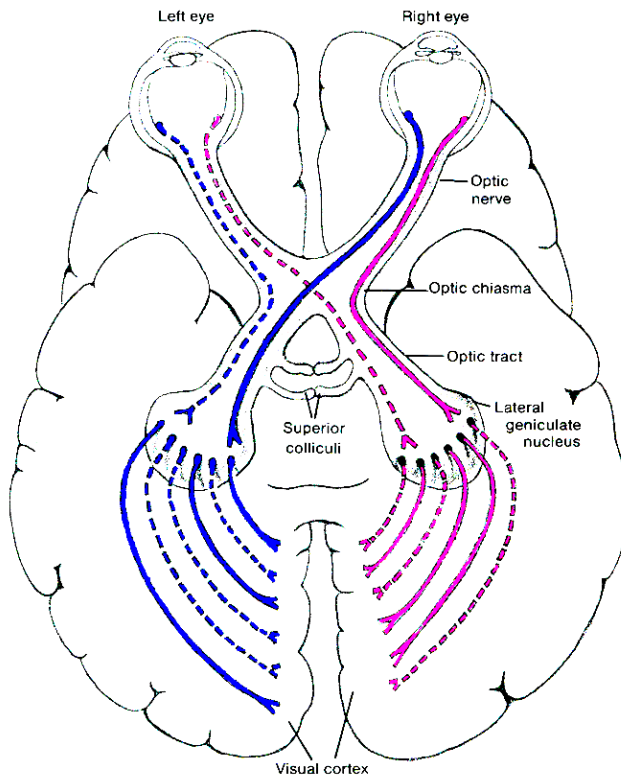


**Figure 3. Structure of the mammalian visual system.** Retinal ganglion cells from both eyes project to the thalamic lateral geniculate nucleus. Partial crossing of the two pathways occurs in the optic chiasm. Neurons of the lateral geniculate nucleus project to the visual cortex in the occipital lobes where neurons form eye-specific patches, ocular dominance columns. Image source: World Wide Web (<http://www.skidmore.edu/~hfoley/Perc3.htm>).

Although the development of both LGN and V1 is dependent on spontaneous retinal activity, visual activity is also required for their proper maturation. Blocking retinal activity of one eye during the development of the visual circuits while leaving the other one intact leads to the perturbation of the segregation of LGN neurons into eye-specific layers (Shatz, 1996). In the visual cortex, ODCs do not form properly if one eye is deprived of input. As a consequence of visual deprivation, the ODCs display a shift towards the increase of the fraction of neurons responsive to the intact eye (Berardi et al., 2003; Sur et al., 2005). Furthermore, neurons receiving afferents from the intact eye tend to expand their synaptic space and

occupy more territory within the visual cortex. On the other hand, neurons receiving afferents from the deprived eye shrink their territory (Figure 4, Berardi et al., 2003).

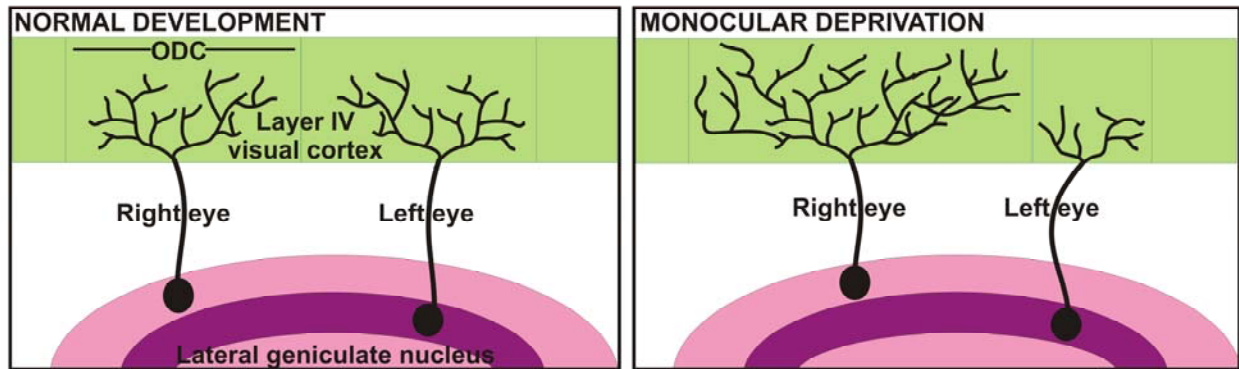


**Figure 4. Effects of monocular deprivation on visual cortex development.** Normal development of the visual cortex is based on the competition between the two eyes which confers balanced development of lateral geniculate nucleus (LGN) neurons and their connections with the visual cortex neurons in ocular dominance columns (ODCs; left part of the figure). If one eye is deprived of visual input throughout the development of the visual system, LGN neurons receiving afferents from the deprived eye shrink and prune their connections in the visual cortex (right part of the figure). This also causes shrinkage of ODCs in the visual cortex that receive input from the deprived eye (in the figure: left eye). On the other hand, ODCs receiving input from the intact eye, expand their territory within the visual cortex (in the figure: right eye).

The first studies highlighting the neuronal expression of MHCI revealed an essential role for MHCI genes in the segregation of retinal inputs and neuronal layers in the LGN (Corriveau et al., 1998; Huh et al., 2000). Functional studies of MHCI-deficient mice have suggested an important role for MHCI molecules in synaptic refinement. MHCI-deficient mice display an aberrant development of retinal projections and impairments in the formation of eye-specific regions in the LGN, which is caused by an excess of inappropriate synapses that are normally removed during LGN development in wild-type mice (Huh et al., 2000). These studies implicated MHCI in the weakening, removal and pruning of synapses,

and it is believed that MHC I limits plasticity in the developing visual system (Syken et al., 2006).

## 1.6. MHC class I molecules in the hippocampus

The hippocampus is a part of the brain situated in the medial temporal lobe implicated in learning and memory processes. It is one of the best studied circuits within the brain, which makes it amenable for various plasticity studies. Hippocampus is organized as a series of connected cell layers: the dentate gyrus, hilus, and cornu ammonis 1, 2 and 3 (CA1-3). The dentate gyrus is composed of granule cells that receive input from the entorhinal cortex and send projections to the hilus and the CA3 pyramidal neurons region. The dentate gyrus to hilus and CA3 projections are known as the mossy fiber pathway (Figure 5). The CA3 pyramidal neurons innervate the CA1 cell layer, and the CA1 pyramidal neurons in turn send output to the entorhinal cortex. The CA3 to CA1 connections are also called Schaffer collaterals.

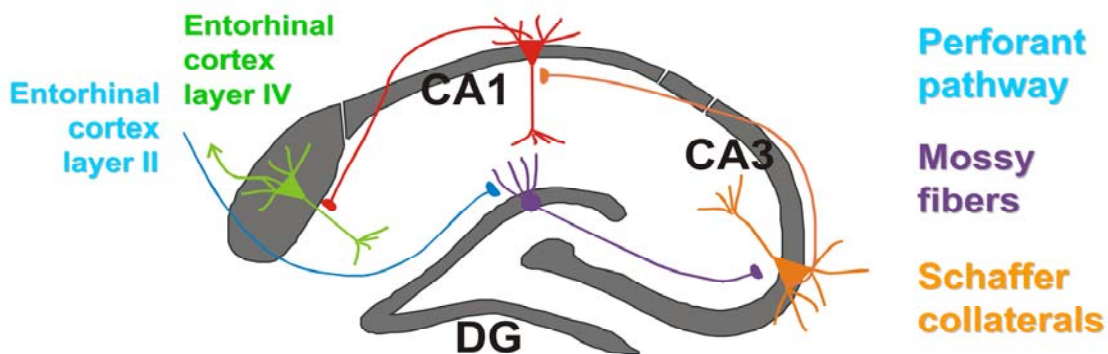


**Figure 5. Schematic structure of the hippocampus.** Granule cells in the dentate gyrus (DG) receive input from the entorhinal cortex (blue) and send their projections to the CA3 pyramidal neurons (*mossy fiber pathway*; purple). CA3 neurons innervate CA1 pyramidal neurons (*Schaffer collaterals*; orange), which in turn send their projections back to the entorhinal cortex (red).

MHCI proteins in mice have been shown to be localized to the somata and dendrites of the dentate gyrus granule neurons and the CA1-CA3 pyramidal neurons. It has been demonstrated that MHCI localizes to the postsynaptic sites in the hippocampal neurons, and MHCI-deficient mice displayed abnormalities in synapse structure as well as in basal synaptic transmission in hippocampal neurons (Goddard et al., 2007). Long term potentiation (LTP) and long term depression (LTD) are two forms of plasticity manifested in long lasting strengthening and weakening of synapses, respectively, and are implicated in learning and memory formation in the hippocampus. Both LTP and LTD are aberrant in mice lacking MHCI molecules (Huh et al., 2000). The exact mechanism of MHCI action in the hippocampus is not fully clear. However, it has been shown that MHCI deficient mice are unable to exhibit LTD in the hippocampus. LTP is significantly enhanced in these mice which parallels the effects of MHCI in the visual system: LTP reflects strengthening of the neuronal connections and the absence of MHCI causes strengthening of synapses that would otherwise be weakened by LTD.

### **1.7. The common marmoset as a model system**

The common marmoset (*Callithrix jacchus*) is a New World monkey that has become a very useful model in the research of visual system development (Fonta et al., 2000). Marmoset monkeys have a small body size and are easy to breed and handle. They display some peculiarities throughout postnatal development of their visual cortex. All primates investigated thus far display three main stages of synaptogenesis during postnatal development of the cortical visual area V1: the initial/early stage, the peak stage (when the number of synapses may reach very high values), and the stage of rapid synapse reduction

(when excess synapses are eliminated and synapse density is normalized to adult levels) (Missler et al., 1992 and 1993; Bourgeois and Rakic, 1993). In the marmoset visual cortex, the number of synapses present during the peak stage may reach a level that is almost double that of the adult value (Missler et al., 1992 and 1993). This provides a nearly perfect platform for investigating levels of MHCII expression throughout the primate visual system development. Furthermore, the structure of the marmoset hippocampus closely resembles that of humans and the relatively small size of the marmoset brain makes them well suited for functional studies (Seress, 2007).

## 1.8. Aims of the study

Although MHCI genes are well conserved among mammals, there are a number of differences in the organization, structure, and function of these genes between rodents and primates (Kumanovics et al., 2003, Kelley et al., 2005). Areas with particularly strong MHCI gene expression across all species are the hippocampal formation, substantia nigra, and the neocortex. MHCI genes of the common marmoset are not well characterized (Cadavid et al., 1997) but our group has previously demonstrated the expression of several MHCI genes in neurons of the adult common marmoset monkeys (*Callithrix jacchus*) that reveals a pattern comparable to that observed in other mammals (Rölleke et al., 2006). The present thesis addresses the question whether in the primate brain, MHCI may be associated with synapse formation and may play a role in the functioning of synapses. Therefore, the spatiotemporal pattern of expression of MHCI genes in the visual system of the marmoset monkey was investigated at different developmental stages. Furthermore, the expression pattern and properties of MHCI in the hippocampus were also studied. The hippocampus is well characterized in all common model animals including primates, but displays some structural differences between rodents and primates (Seress, 2007). This study revealed inter-species differences in MHCI spatiotemporal expression pattern in the visual cortex, as well as differences between mice and marmosets in localization and properties of MHCI in the hippocampus.

## 2. Materials and methods

### 2.1. Animals

Thirty three common marmoset monkeys (*Callithrix jacchus*, 31 males, 2 females) were investigated. The animals were obtained from the breeding colony at the German Primate Center (Göttingen, Germany). All animal experiments were conducted in accordance with the European Communities Council Directive of November 24, 1986 (86/EEC) and with the National Institutes of Health Guide for the Care and Use of Laboratory Animals, and were approved by the Lower Saxony Federal State Office for Consumer Protection and Food Safety under reference numbers 33.42502-04-026/07 and 33.11.42502-04-003/08.

The following animal ages were used for expression studies (staged according to Missler et al., 1992 and 1993): postnatal days 1 and 7; and postnatal months 1, 3, 5, 7, 12, and 21. For monocular enucleation (ME), the left eyes of six one-month-old marmoset monkeys (with an approximate weight of 75 g) were surgically enucleated under general anesthesia. As anesthesia, the animals received 0.1 ml of a premix containing 4 mg/ml alphaxalon and 1.33 mg/ml alphadolon (Saffan®; Schering-Plough Animal Health, Welwyn Garden City, UK), 0.37 mg/ml diazepam, and 0.015 mg/ml glycopyrroniumbromid (Robinul®; Riemser, Germany). Enucleation was carried out as described for pet animals (Schebitz and Brass, 2007). The cavity was filled with gelastyp® sponge (Sanofi-Aventis, Germany) as soon as arterial bleeding was no longer visible. The wound was closed with an intracutane suture of vicryl 6-0 (V302H; Ethicon, Germany). After surgery (day 0) and on days 3 and 5, all animals received an antibiotic treatment of amoxicillin–trihydrate (Duphamox LA®, Fort Dodge, Germany). Animals were sacrificed at five months of age. For electrophysiology,

animals were 2, 4 and 5 years old. In all cases the minimum number of animals required to obtain consistent data was used.

## **2.2. Brain sections**

For *in situ* hybridization, brains were immediately removed from terminally anesthetized animals [overdose of ketamine (50 mg/ml), xylazine (10 mg/ml), and atropine (0.1 mg/ml)]. The visual cortex and temporal lobes were quickly dissected, embedded in Tissue Tek (Sakura Finetek, Heppenheim, Germany), flash frozen in liquid nitrogen, and stored at –80°C. Frozen brains were sectioned using a cryostat (Leica CM3050, Bensheim, Germany) and coronal sections (10 µm) of visual cortex and medial temporal lobes were thaw-mounted on adhesive saline-coated slides (Marienfeld, Laboratory Glassware, Lauda-Königshofen, Germany). For immunohistochemistry, marmosets that had been terminally anesthetized with an overdose of ketamine (50 mg/ml), xylazine (10 mg/ml), and atropine (0.1 mg/ml) were perfused transcardially with 0.9% saline, followed by 200 ml of fixative containing 4% paraformaldehyde in 0.1 M sodium–phosphate buffer (pH 7.2) for 15 min. Animal heads were postfixed using the same fixative and the brains were carefully removed from the skull on the following day. After cryoprotection with 0.1 M phosphate-buffered saline (PBS; 0.1 mM phosphate buffer, 0.9% NaCl, pH 7.2) containing 30% sucrose (for at least 48 h), serial coronal sections (thickness: 40 µm for expression studies and 60 µm for monocularly enucleated animals) were obtained using a cryostat.

### 2.3. PCR cloning of MHC class I transcripts

The isolation of the common marmoset MHCI cDNA sequences was carried out using reverse transcriptase polymerase chain reaction (RT-PCR). One microgram of total brain RNA was reverse transcribed using the oligo (dT) primer GACTCGAGTCGACATCGA(T)<sub>17</sub> and 400 U of reverse transcriptase (Promega, Mannheim, Germany). An aliquot of this reaction was used as a template in a PCR containing primers designed using the Primer3 software (Rozen and Skaletsky, 2000), which were devised to amplify full-length marmoset MHCI transcripts. Primer sequences included BamHI restriction sites and were as follows: forward 5'-CACGGATCCCACTTTACAAGCCGTGAGAGAC-3', reverse 5'-CACGGATCCCTCCTGTTGCTCTCGGGGGCCTTG-3'. Caja-G\*1 (accession number: U59637) was obtained by amplification with *Taq* polymerase and cloned into the pDrive vector (Qiagen) following manufacturers instructions. The construct was propagated in Top10 competent cells (Invitrogen), plasmid DNA was isolated using QIAprep Miniprep kit (Qiagen) and sequenced using BigDye Terminator (Applied Biosystems), all following manufacturers instructions *Pfu* polymerase (Fermentas GmbH, Germany) was also used for amplification and subsequent cloning into pEXPR103 (IBA Technologies, Germany).

### 2.4. In situ hybridization

Cryosections (10 μm) of visual cortex and the hippocampus were dried at RT for 20 min, fixed in 4% buffered paraformaldehyde (PFA, pH 7.2), rinsed in PBS, acetylated (0.1 M triethanolamine, 0.25% acetic anhydride), washed in PBS, and dehydrated through a graded ethanol series. Caja-G plasmid DNA was linearized and riboprobes were synthesized using T7 and SP6 RNA polymerases (Promega, Madison, WI, USA) for the

antisense and sense probe, respectively, in the presence of 9.25 MBq of  $^{33}\text{P}$ -UTP (Hartmann Analytic GmbH, Braunschweig, Germany; specific activity, 3,000 Ci/mmol) for 1 h at 37°C. Probes were purified using Microspin S-400 HR columns (Amersham Pharmacia, Freiburg, Germany) and hybridization buffer (50% deionized formamide, 10% dextran sulphate, 0.3 M NaCl, 1 mM EDTA, 10 mM Tris-HCl, pH 8.0, 500  $\mu\text{g/ml}$  tRNA, 0.1 M dithiothreitol, and 1  $\times$  Denhardt's solution) was added to yield a final probe activity of  $5 \times 10^4$  CPM. The hybridization mixture containing the probe was denatured at 70°C for 10 min, cooled to 55°C, and pipetted directly onto the sections (80  $\mu\text{l}$ /section). Hybridization was performed for 18 h at 68°C. Sections were subsequently washed in 4  $\times$  SSC (0.6 M NaCl, 0.06 M citric acid), 2  $\times$  SSC, and 0.5  $\times$  SSC for 10 min each at 37°C. After a one hour incubation at 75°C in 0.2  $\times$  SSC for Caja-G and 47°C for  $\beta$ -2-microglobulin, sections were washed twice in 0.1  $\times$  SSC, once at 37°C and again at RT, for 10 min each. Sections were dehydrated through graded alcohols, air dried, and exposed to Bio-Max MR film (Amersham Pharmacia) for three days at 4°C. Films were developed and fixed with GBX (Kodak, Rochester, NJ, USA).

## **2.5. Quantitative in situ hybridization**

After hybridization (described above), sections were coated with photoemulsion (Kodak NBT) at 42°C, dried for 90 min at RT, and stored for seven weeks at 4°C in a lightproof container. Exposed slides were developed at 15°C for 5 min (Kodak developer D-19), rinsed twice briefly in  $\text{H}_2\text{O}$ , and fixed for 5 min at RT (Kodak Polymax). Sections were counterstained with 0.05% toluidine blue in 0.1% disodium tetraborate (Sigma) for

expression studies and with methyl green (Sigma) for sections from ME animals, cleared in xylol, and coverslipped with mounting medium (Eukitt, Kindler, Freiburg, Germany). Hybridized sections were visualized with a 40 × objective (NA = 1.4; Zeiss) under a light microscope (Axioscope, Zeiss) and silver grain quantification was performed on a cell-by-cell basis using ImageJ (Abramoff et al., 2004). Images were obtained from layer IV neurons and, for each area of interest two images were acquired, i.e., one using a green filter to eliminate background interference from methyl green and one using white light to later precisely localize neuronal nuclei. A circular counting mask that corresponded to 15 μm was used to delineate the region of interest and was placed over neuronal nuclei during counting. Relative optical density (ROD) threshold intensities were optimized to detect exposed silver grains exclusively. The intensity of pixels present within the region of interest was measured. Grain counts (number of grains/cell) were compared between the left and right hemispheres of three animals (three slides per animal, approximately 400 neurons per animal were counted). Pixel intensities of detected silver grains were compared between left and right hemispheres using a Student's *t* test (GraphPad Prism version 4 for Windows, GraphPad Software, San Diego, California, USA).

## **2.6. Quantitative RT–PCR**

To isolate RNA for RT–PCR, brains were immediately removed from terminally anesthetized animals [overdose of ketamine (50 mg/ml), xylazine (10 mg/ml), and atropine (0.1 mg/ml)] and were quickly dissected. Total RNA was isolated from individual visual cortex samples using the QIAGEN RNeasy kit (Qiagen) according to the manufacturer's instructions. The integrity and quantity of the purified RNA was assessed by spectrophotometry.

Complementary DNA (cDNA) was synthesized from mRNA transcripts using oligo (dT)<sub>12-18</sub> primers and Superscript II reverse transcriptase (Invitrogen, Karlsruhe, Germany), according to the manufacturers' instructions. The Primer3 software v2.0 (Rozen and Skaletsky, 2000) was used to design gene-specific primers, with amplicons ranging from 50 to 150 bp in length. The primers used for the detection of MHCI transcripts were: forward 5'-GTGATGTGGAGGAAGAACAGC-3', reverse 5'-CACTTTACAAGCCGTGAGAGA-3' (accession number U59637). Primers for the detection of  $\beta$ -actin were: forward 5'-CATCCGCAAAGACCTGTATG-3', reverse 5'-GGAGCAATGACCTTGATCTTC-3' (accession number DD279463). A quantitative analysis of gene expression was performed using the 7500 Real-time PCR apparatus (Applied Biosystems, Darmstadt, Germany) in combination with Quantitect SYBR green technology (Qiagen). The light cycler was programmed to the following conditions: an initial PCR activation step of 10 min at 95°C, followed by 40 cycles (denaturation for 15 s at 95°C, annealing for 30 s at 55°C, and elongation for 60 s at 72°C). Details of the quantitative real-time PCR were described previously (Abumaria et al., 2008). Dissociation curves were generated for all PCR products to confirm that SYBR green emission was detected from a single PCR product (Ririe et al., 1997). The relative abundances of the MHCI mRNA transcripts were calculated relative to the mRNA levels of the internal reference gene  $\beta$ -actin and were compared between cortices using a Student's *t* test (GraphPad Prism version 4 for Windows).

## **2.7. Immunocytochemistry for light microscopy**

Coronal cryosections (40  $\mu$ m for expression studies and 60  $\mu$ m for ME animals) from the visual cortex were collected and washed briefly in PBS before the epitope retrieval step.

Epitope retrieval was performed by incubating the sections for 20 min in 10 mM sodium citrate buffer preheated to 80°C. Sections were later brought to RT, washed in PBS, and quenched of endogenous peroxidase activity using a 30 min incubation at RT in 0.5% H<sub>2</sub>O<sub>2</sub> in distilled water. Sections were then washed in PBS, blocked for 1 h at RT (3% normal horse serum in PBS), incubated for 16 h at 4°C with monoclonal TP25.99 IgG (kindly provided by S. Ferrone; 1:300 dilution in 3% normal horse serum in PBS), monoclonal rabbit anti c-Fos (1:200 dilution in 0.03% Triton-X-100 and 3% normal horse serum in PBS, Cell Signaling Technologies) or with control mouse IgG (Sigma), and washed again. Sections were then incubated with biotinylated horse anti-mouse IgG or donkey anti-rabbit (Vector Laboratories, 1:200 dilution in 3% normal horse serum in PBS) for 1 h at RT. After washing, sections were incubated with avidin-biotin horseradish peroxidase (Vectastain Elite ABC Kit, Vector Laboratories, USA; 1:100 dilution in 3% normal horse serum in PBS) for 1 h at RT, washed in PBS and then again in 0.05 M Tris/HCl (pH 7.2) prior to DAB detection (DAB detection with nickel enhancement was performed according to the manufacturer's instructions; DAB-Kit, Vector Laboratories). For contrast enhancement, sections from enucleated animals were incubated with DAB for shorter periods. Sections were washed in 0.05 M Tris/HCl (pH 7.6) and again in 0.1 M PBS prior to xylol clearance, dehydration, and coverslipping with Eukitt mounting medium (Kindler). Cytochrome oxidase (CO) detection was performed as previously described (Wong-Riley, 1979; Spatz et al., 1994). Briefly, sections were washed in phosphate buffer (0.1 M, pH 7.4), incubated at 40°C in a mixture of phosphate buffer, cytochrome C oxidase (Sigma), sucrose (Sigma), and the chromogen DAB (Sigma). Sections were kept in this solution for approximately 4 h or until a CO reactive band in layer IV was visible. Sections were then dehydrated in a series of graded alcohols, cleared in xylol, and coverslipped with Eukitt mounting medium (Kindler).

For hippocampus, coronal cryosections (40  $\mu\text{m}$ ) were collected from marmoset brain sections containing the hippocampal formation and washed briefly in PBS and quenched of endogenous peroxidase activity by 30 min incubation at RT in 0.5%  $\text{H}_2\text{O}_2$  in distilled water. Sections were rinsed in PBS, blocked for 1 hr at RT (3% normal horse serum and 0.03% Triton-X-100 (Sigma) in PBS), incubated 16 hrs at 4°C with either monoclonal HCA2 IgG (1 mg/ml, 1:500 dilution in 3% normal horse serum and 0.03% Triton-X-100 (Sigma) in PBS), or with control mouse IgG (Sigma), and washed again. Sections were then incubated with biotinylated horse anti-mouse IgG (Vector Laboratories, 1:200 dilution in 3% normal horse serum and 0.03% Triton-X-100 (Sigma) in PBS) for 1 hr at RT. After washing, sections were incubated with avidin-biotin-horseradish peroxidase (Vectastain Elite ABC Kit, Vector Laboratories, USA; 1:100 dilution in 3% normal horse serum and 0.03% Triton-X-100 (Sigma) in PBS) for 1 hr at RT, washed in PBS and then again in 0.05 M Tris/HCl (pH 7.2) prior to DAB detection (DAB detection with or without nickel enhancement was performed according to the manufacturer's instructions; DAB-Kit, Vector Laboratories). For immunocytochemistry with HC10 antibody, epitope retrieval step was performed prior to all other steps. Sections were later processed as described above for epitope retrieval and incubated in monoclonal HC10 (1 mg/ml, 1:500 dilution in 3% normal horse serum in PBS).

For Timm's stain, hippocampal slices (1 mm) were immersed in 0.4%  $\text{Na}_2\text{S}$  for 30 min, and then fixed for 16 hr in 1% paraformaldehyde and 1.25% glutaraldehyde. The fixed slices were cryoprotected, 30  $\mu\text{m}$  sections were mounted and dried, and sections were immersed in developer consisting of 30 ml gum Arabic (50%), 5 ml citrate buffer (2 M, pH 3.7), 15 ml hydroquinone (5.67%) and 0.25 ml  $\text{AgNO}_3$  (17%) for at least 60 min. Digital images of immunostained tissue sections were acquired using Axiophot II microscope (Zeiss). Final

images were assembled in Corel PHOTO-PAINT X3 and are a composition of 4-6 images encompassing the entire hippocampal formation.

## **2.8. Immunofluorescence and confocal microscopy**

Antibodies used in double-labeling experiments were applied sequentially and blocking steps were performed using normal sera of the host species from which the respective secondary antibodies were derived. For visual cortex, cryostat sections (40  $\mu\text{m}$ ) were rinsed in PBS before the epitope retrieval step was performed, as described above. Nonspecific antibody binding sites were blocked with 3% normal serum in PBS for 1 h at RT. Sections were then incubated with mouse monoclonal TP25.99 antibody (1:300 in 3% normal serum in PBS) for 16 hrs at 4°C, washed, and incubated in secondary antiserum (Alexa 488-coupled goat anti-mouse, Molecular Probes, Invitrogen, Leiden, Netherlands) at a dilution of 1:500 for 4 h in a lightproof container. Sections were washed and incubated with rabbit anti-MAP2, rabbit anti-SAP102, rabbit anti-gephyrin, rabbit anti-vimentin or rabbit anti-GFAP (dilutions provided in Table 1) in 3% normal serum in PBS for 16 h at 4°C. Sections were then washed and incubated 4 h at RT in secondary antiserum (Alexa 568-coupled goat anti-rabbit, Molecular Probes, Invitrogen) diluted 1:500 in PBS.

For the hippocampus, cryostat sections (40  $\mu\text{m}$ ) of marmoset brains containing the hippocampal formation were rinsed in PBS. Non-specific antibody binding sites were blocked with 3% normal serum and 0.03% Triton-X-100 (Sigma) in PBS for 1 hr at room temperature. Sections were then incubated in mouse monoclonal HCA2 for marmoset sections [1/500 in 3% normal serum and 0.03% Triton-X-100 (Sigma) in PBS] for 16 hrs at

4°C, washed, and incubated in secondary antiserum (Alexa 488-coupled goat anti-mouse, Molecular Probes, Invitrogen, Leiden, Netherlands) dilution 1:500 for 4 hr in a light proof container. Sections were washed and incubated in either rabbit anti-SAP102, rabbit anti-piccolo, rabbit anti-VGluT1 or rabbit anti-VGluT2 (dilutions provided in Table 1) in 3% normal serum and 0.03% Triton-X-100 (Sigma) in PBS for 16 hrs at 4°C. Sections were then washed and incubated 4 hrs at room temperature in secondary antiserum (Alexa 568-coupled goat anti-rabbit, Molecular Probes, Invitrogen) diluted 1:500 in PBS. Thereafter, sections were washed in PBS and floated/mounted on Histobond slides in distilled water, allowed to dry overnight at 4°C, and coverslipped with mounting medium (Aqua-Polymount, Polysciences Inc., USA). Confocal microscopy was performed using a laser-scanning microscope (LSM 5 Pascal, Zeiss) with an argon 488 nm laser and a helium/neon 543 nm laser. Analyses were performed in multiple-tracking mode, to avoid bleed-through between channels. The 543 nm laser was always used with a smaller detection pinhole diameter than that of the 488 nm laser, to obtain the same optical slice thickness (slice thickness was typically between 0.5 and 1.0  $\mu\text{m}$ ). High magnification, single optical plane images of layer IV neurons of the visual cortex were obtained at a resolution of 1,024x1,024 with an Apochromat 63x oil objective (NA = 1.4) and immersion oil (Immersionol, Zeiss; refractive index = 1.518). For quantitative immunofluorescence, high magnification images as z-series stacks of the mossy fiber terminals region or of layer IV in the visual cortex in 1024x1024 resolution were obtained with an Apochromat 63x oil objective (NA = 1.4) and immersion oil (Immersionol, Zeiss; refractive index = 1.518). For quantification of colocalization, the intensity correlation coefficient (Li et al., 2004) was obtained with ImageJ colocalization plugin (Abramoff et al., 2004) for a minimum of three images per animal and compared between

two groups using Student's *t*-test (GraphPad Prism version 4 for Windows). The region of interest (ROI) was defined with the green channel (MHC1 signal).

<b>3<sup>rd</sup> antibody (marker)</b>	<b>Dilution</b>	<b>Supplier</b>
Gephyrin	1:200	Abcam
GFAP	1:500	SySy
MAP2	1:200	SySy
Piccolo	1:200	SySy
VGlut1	1:2000	SySy
VGlut2	1:200	SySy
Vimentin	1:200	SySy

**Table 1. List of antibodies used for detection of neuronal, glial and synaptic markers and the dilutions used.**

## **2.9. Protein extraction**

Brains were immediately removed from the terminally anesthetized animals [by an overdose of ketamine (50 mg/ml), xylazine (10 mg/ml), and atropine (0.1 mg/ml)]. Samples of hippocampi and visual cortex were homogenized with a Dounce homogenizer (tight pestle) in ice-cold homogenization buffer consisting of 50 mM Tris/HCl pH 7.4, 7.5% glycerol, 150 mM NaCl, 1 mM EDTA, 1% Triton-X 100, and complete protease inhibitor cocktail (Roche Diagnostics, Mannheim, Germany). After homogenization, the samples were centrifuged at  $4,000 \times g$  for 20 min at 4°C. The resulting supernatant was centrifuged again until it was clear. Protein concentration was measured using the Bio-Rad DC Protein assay (Bio-Rad Laboratories, Hercules, USA).

## **2.10. Antibody purification and dialysis**

Monoclonal HCA2 and HC10 antibodies were purified from HCA2 and HC10 hybridoma supernatants (kindly provided by B. Uchanska-Ziegler, Freie University Berlin, Germany) using Protein G Sepharose (GE Healthcare, Munich, Germany) following the manufacturer's instructions. Antibodies were later dialyzed with Amicon concentrators (Milipore, Billerica, MA, USA) against sterile 0.1 M PBS.

## **2.11. Immunoblot analysis**

Protein preparations were electrophoresed in 12.5% SDS gels under reducing conditions. Proteins were subsequently transferred to nitrocellulose membranes (Schleicher and Schuell, Dassel, Germany) via semidry electroblotting for 2 h at 1 mA/cm<sup>2</sup> in transfer buffer containing 25 mM Tris base, 150 mM glycine, and 10% (v/v) methanol. After the transfer, blots were blocked with 5% (w/v) milk powder and 0.1% Tween-20 in PBS for 1 h at RT and were then incubated with either monoclonal TP25.99 for visual cortex proteins, HCA2 and HC10 for the hippocampal proteins (all used at 1:1,000 dilution) or monoclonal anti-SNAP-25 (1:1,000, Synaptic Systems) antibodies overnight at 4°C. After washing three times for 5 min in PBS/0.1% Tween-20, blots were incubated for 1 h at RT with horseradish peroxidase-coupled goat anti-mouse IgG (1:4,000, Santa Cruz Biotechnology, Santa Cruz, USA). Prior to visualization, blots were washed in PBS/0.1% Tween-20 (3 × 5 min) and once more in PBS. Signals were visualized using SuperSignal West Dura enhanced luminescence substrate (Pierce Biotechnology, Rockford, USA). Membranes were subsequently stripped in a mixture of β-mercaptoethanol in PBS and incubated with monoclonal anti-β-actin antibody (1:4000, Sigma). For quantification, blots were visualized

so that nonsaturating bands were obtained. Quantification was performed using the gel analysis plug-in of ImageJ.

## **2.12. Image analysis of sections from monocularly enucleated animals**

Digital images of immunostained tissue sections were acquired using an Axiophot II microscope (Zeiss). Images were taken from right visual cortices. Variations in MHCI immunoreactivity through layer IV were measured as described previously (Catalano et al., 1997). Briefly, images were normalized and regions within layer IV that encompassed the thickness of the entire layer IV (2 mm in length and approximately 0.25 mm in thickness) were defined as the regions of interest. The vertical staining profile was obtained using ImageJ. Values were averaged (using the four closest neighbors) and plotted as a function of the distance along layer IV parallel to the pia mater. After delineating the borders of immunoreactive patches, their width was measured using ImageJ and compared using a Student's *t* test (GraphPad Prism version 4 for Windows).

## **2.13. Cell culture, immunoprecipitation and protein purification**

HEK293T cells were transfected with linearized, full-length Caja-G carrying a C-terminal StrEP-tag in pEXPR-IBA103 (IBA Technologies, Göttingen, Germany) using Fugene 6 (Roche, Indianapolis, IN, USA) as described by the manufacturer. Stable clones were selected with Geniticine (G418, Life Technologies, Karlsruhe, Germany) and further propagated. Protein extracts were obtained as described above. Purified Caja-G carrying a C-terminal StrEP-tag was obtained following the manufacturer's protocol (IBA Technologies,

Göttingen, Germany). For immunoprecipitation, 1 mg/ml of protein extract was precleared with Protein G Sepharose Fast Flow (GE Healthcare) for 1 hour at 4°C. Samples were centrifuged briefly and the supernatants were incubated with either monoclonal HCA2 IgG (1:300) or monoclonal HC10 IgG (1:300) or without antibodies overnight on a rotary platform at 4°C. Samples were then centrifuged and pellets were washed 3 times with lysis buffer [50 mM Tris/HCl pH 7.4, 150 mM NaCl, 1 mM EDTA, 1% Triton-X 100 and complete protease inhibitor cocktail tablet (Roche Diagnostics, Mannheim, Germany)]. The bound proteins were eluted by boiling in Laemmli buffer (Laemmli, 1970) and Western blot was performed as described above. After transfer, the blot was blocked with 5% (w/v) BSA (Sigma) and 0.1% Tween-20 in PBS for 1 h at room temperature, and then incubated with monoclonal anti-StrEP HRP-conjugated antibody (1/4000 dilution, IBA Göttingen, Germany) overnight at 4°C. After washing three times for 5 min in PBS/0.1% Tween and once more in PBS, signals were visualized by SuperSignal West Pico enhanced luminescence substrate (Pierce Biotechnology, Rockford, USA).

## **2.14. Electrophysiology**

Whole cell patch clamp technique enables recordings of ion flow through the membrane of the patched cells. The current flowing through the membrane is measured while the cell membrane potential is held constant. The flow is detected with an electrode placed in a glass pipette that is in contact with the intracellular solution. Signal obtained is amplified and digitized which enables its later analysis.

For acute slices preparation, animals were terminally anesthetized with an overdose of ketamine (50 mg/ml), xylazine (10 mg/ml), and atropine (0.1 mg/ml) and were intracardially

perfused with ice-cold oxygenated (95% O<sub>2</sub> and 5% CO<sub>2</sub>) modified artificial cerebrospinal fluid (ACSF) containing (in mM): sucrose, 220; KCl, 1.9; Na<sub>2</sub>HPO<sub>4</sub>, 1.25; glucose, 10; NaHCO<sub>3</sub>, 33; MgCl, 26; CaCl<sub>2</sub>, 20.5; kynurenic acid, 2; and ascorbic acid, 2 (all from Sigma). Transverse hippocampal slices (300–400 μm) were prepared using a vibroslicer (752 M, Campden Instruments, Loughborough, UK), transferred to the recording chamber, and allowed to recover at 33°C for at least 90 min, after which they were kept at room temperature. Recordings were performed on slices placed in a submerged chamber perfused with oxygenated ACSF (33°C) containing (in mM): NaCl, 124; KCl, 5; Na<sub>2</sub>HPO<sub>4</sub>, 1.25; glucose, 10; NaHCO<sub>3</sub>, 26; MgSO<sub>4</sub>, 2; CaCl<sub>2</sub>, 2; and ascorbic acid, 1 (all from Sigma). The recording chamber was continuously perfused with ACSF and aerated with 95% O<sub>2</sub> and 5% CO<sub>2</sub> (2–3 ml/min). The temperature was kept at 33°C. CA3 neurons were visually identified using an infrared microscopy. The pipette solution contained (in mM): potassium gluconate, 135; MgCl<sub>2</sub>, 2; CaCl<sub>2</sub>, 0.1; EGTA, 1; Na<sub>2</sub> ATP, 2; and HEPES, 10. Spontaneous glutamatergic excitatory postsynaptic currents (EPSCs) were recorded in the presence of 1 μM strychnine and 1 μM bicuculline. Either control IgG or a mixture of HCA2 and HC10 antibodies at a concentration of 1.5 mg/ml were directly applied in close proximity to neurons using glass pipettes (Figure 6). The tip size of the pipette, pressure (0.5 mbar), and application time (0.5 s) were kept constant in all experiments. Signals with amplitudes at least twofold above the background noise were selected. Either control IgG or a mixture of HCA2 and HC10 antibodies at a concentration of 1.5 mg/ml was directly applied in close proximity to neurons by glass pipettes and in line with the chamber flow direction (Figure 6). To minimize the variation between experiments, we kept tip size of the pipette, pressure (0.5 mbar), and application time (1 ms) constant for all experiments. In addition, the distances

between pipette tips and the cell were monitored using a camera with a liquid crystal display device and were also kept constant between different experiments (schematic representation of the recording setup is provided in Figure 6). Selected cells were first recorded for three minutes without antibody application (control recording) after which the antibodies were applied at 30 seconds intervals for 20 minutes. Patches with a serial resistance of  $>10\text{ M}\Omega$ , a membrane resistance of  $<0.2\text{ G}\Omega$ , or leak currents of  $>200\text{ pA}$  were excluded. The membrane currents were filtered by a four-pole Bessel filter at a corner frequency of 2 kHz and digitized at a sampling rate of 5 kHz using the DigiData 1322A interface (Molecular Devices). Data acquisition and analysis were done using commercially available software: pClamp 9.0 (Molecular Devices, Sunnyvale, CA), MiniAnalysis (SynptoSoft, Decatur, GA) and Prism 4 for Windows (GraphPad Software, San Diego, CA).

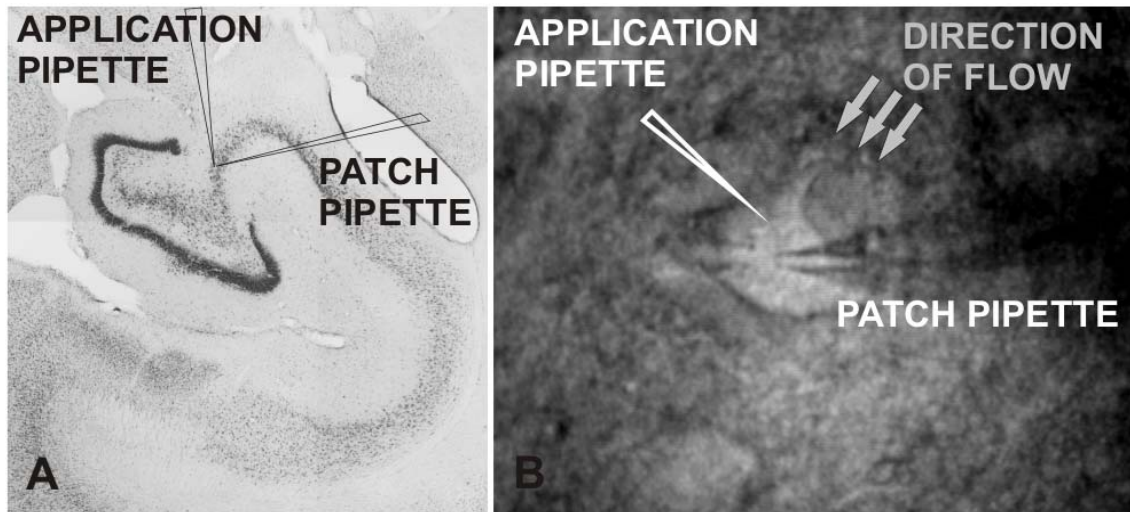


**Figure 6. Schematic representation of the recording chamber setup.** Image on the left is the Nissl stained marmoset hippocampus. Image on the right is one of the recorded marmoset CA3 neurons.

### 3. Results

#### 3.1. Part I: MHC class I molecules in the visual cortex

##### 3.1.1. Expression of MHC I in the visual system of the common marmoset

To investigate the expression of MHC I genes in the marmoset visual system, a full-length clone of the classical marmoset MHC I gene Caja-G (Accession number U59637) was used for *in situ* hybridization experiments. Animals were chosen based on age and according to the main stages of visual system development (Missler et al., 1992 and 1993) and were of the following ages: postnatal days 1 and 7, as well as postnatal months 1, 3, 5, 7, 12, and 21. Since LGN development in primates occurs already *in utero* (Rakic, 1976 and 1977), a strong expression of MHC I genes in newborn animals was expected to be seen, as the expression of these genes persists in adult rodents and cats (Corriveau et al., 1998; Huh et al., 2000). Surprisingly, MHC I signal in the LGN was undetectable, even after long exposures of the autoradiography films, while MHC I mRNA was strongly expressed in hippocampal regions such as the dentate gyrus (Figure 7).

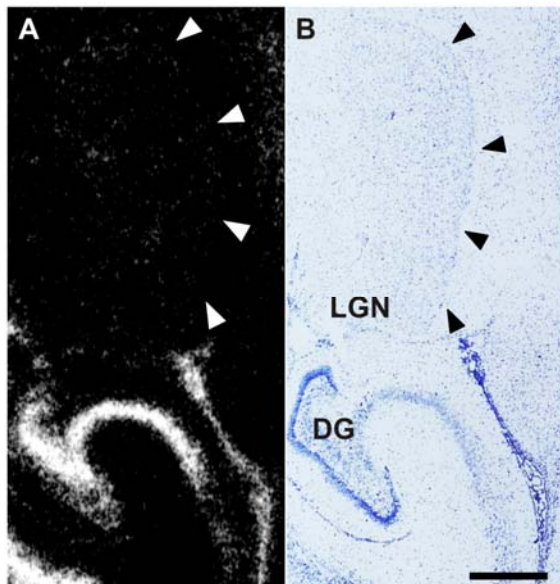


**Figure 7. Lack of MHC class I expression in the lateral geniculate nucleus (LGN) as revealed by *in situ* hybridization.** Autoradiograph of a section processed for *in situ* hybridization (left) and toluidine-blue stained section (right) of a 7 day old marmoset monkey. Note the absence of MHC class I signal in the LGN (delineated with arrowheads). Abbreviations: Dentate gyrus, DG; Scale bar: 1 mm.

However, *in situ* hybridization revealed a strong expression of the MHC I gene throughout the visual cortex. This expression was mainly concentrated in layers I and IV and throughout the subcortical white matter in early postnatal animals (1 and 7 days of age, Figure 8).

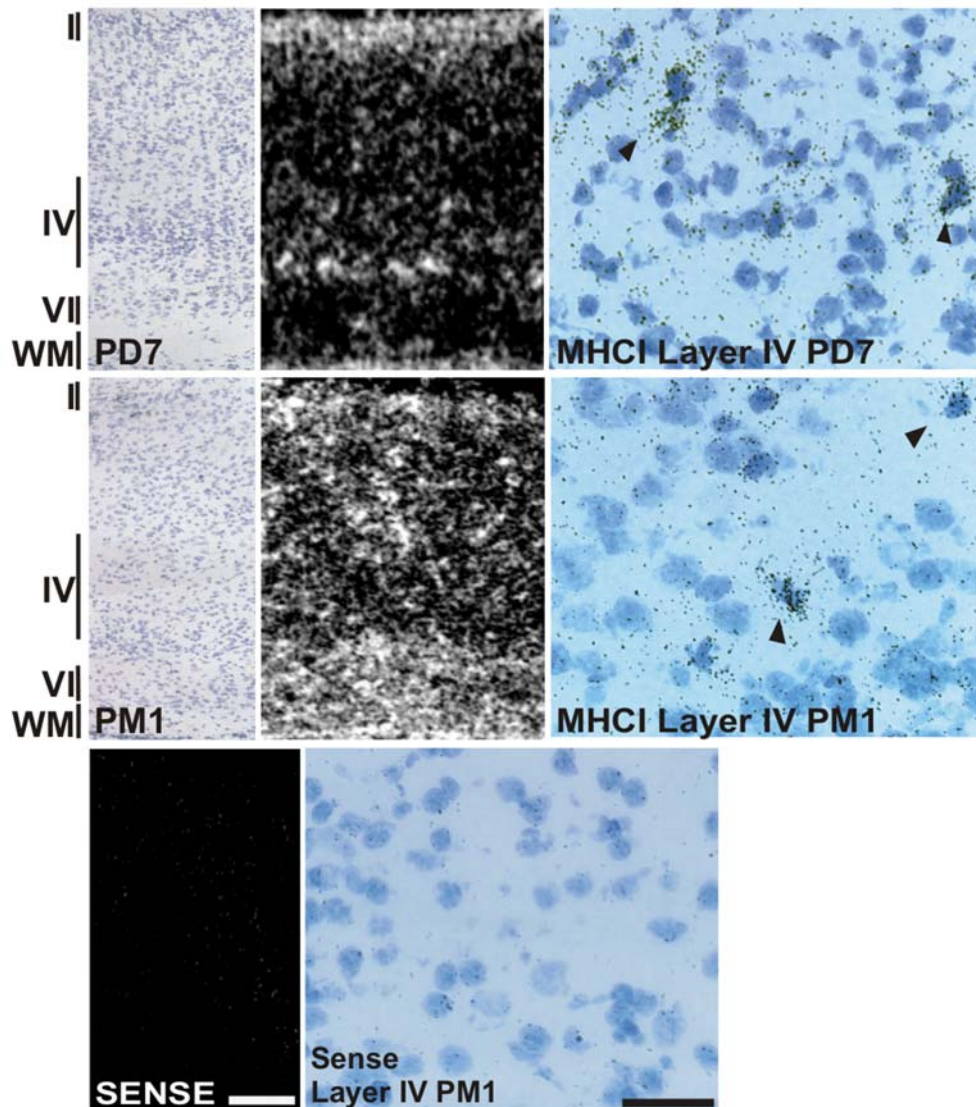


**Figure 8. Expression of MHC class I in the visual cortex as revealed by *in situ* hybridization.**

**Upper row:** Toluidine-blue stained section of a 7 day old animal (left) processed for *in situ* hybridization and autoradiograph of the same section (middle; film autoradiography) reveal strong MHC class I (MHC I) signals in layers I, IV and in the subcortical white matter (WM). Emulsion autoradiography (right) reveal silver grains clustered over single cells (arrowheads). **Middle row:** Toluidine-blue stained section of a 1-month old animal (left) processed for *in situ* hybridization and autoradiograph of the same section (middle) revealed strong, but diffuse MHC class I signals in all cortical layers and in subcortical white matter (WM).

**Figure 8 continued.** Emulsion autoradiography (right) showed silver grains clustered over single neurons (arrows), where a number of neurons were unlabeled (gray arrowhead). **Lower row:** Sense probe revealed only background signals (left; film autoradiograph) and background levels of silver grains in emulsion autoradiography (right). Roman numerals denote cortical layers. Scale bar for film autoradiographs: 1mm. Scale bar for emulsion autoradiography: 20  $\mu$ m.

In older animals (ranging from 1 to 21 months of age), the signal became more diffuse, with cells in all cortical layers exhibiting MHCI gene expression. Nevertheless, expression was strongest in layers IV–VI and in the subcortical white matter (Figure 8). Emulsion autoradiography revealed the presence of silver grains clustered over single cells (Figure 8). The sense probe, which was used as a control, yielded no signal, thus demonstrating the specificity of the MHCI antisense probe (Figure 8).

Antibodies against marmoset MHCI proteins are not available; however, because of the high similarity of these proteins with their human homologues, the well characterized TP25.99 antibody was used for the detection of marmoset MHCI proteins (Woo et al., 1997). The epitope of this antibody lies in the  $\alpha$ -3 domain of MHCI molecules, which is the best conserved domain across all species and is almost identical between marmosets and humans. TP25.99 recognized a band of ~45 kDa in Western blots, which is the expected molecular weight of the MHCI heavy chain. Protein expression was quantified in animals aged one, three, and five months, which represent the main stages of synaptogenesis, namely the initial, peak, and refinement stages (Missler et al., 1993). The expression levels of the MHCI protein coincided with levels of the synaptogenesis marker SNAP-25 (Figure 9).

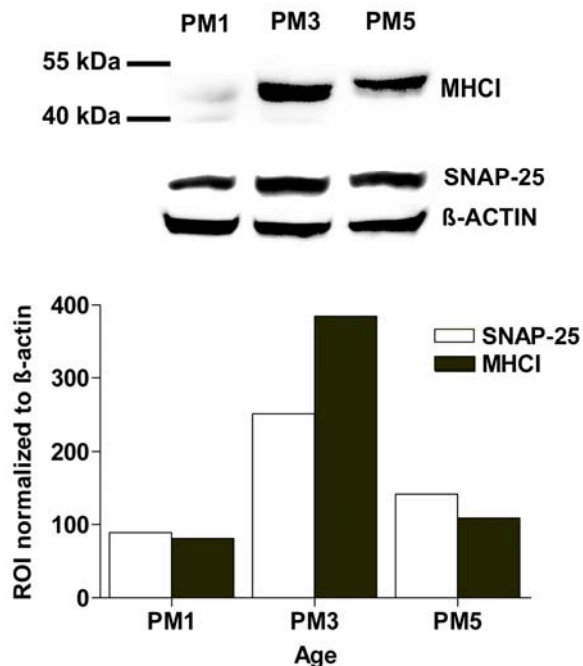


**Figure 9. MHC class I protein levels follow synaptogenesis during visual cortex development.** The antibody TP25.99 (mouse anti-human MHC I) recognized bands of appropriate molecular weight for MHC I in Western blots of proteins extracted from the marmoset visual cortex. Animals were 1, 3 and 5 months old and represent the main stages of synaptogenesis: initial stage, peak and rapid decline/synaptic refinement respectively. SNAP25 was used as a marker of synaptogenesis levels. Data were normalized to  $\beta$ -actin.

Immunocytochemistry revealed a strong staining of neurons throughout the visual cortex in animals of all examined ages (Figure 10). Brain sections adjacent to the ones used for immunocytochemical detection of the MHC I protein were stained for cytochrome oxidase (CO) activity, which is known to be present in neurons of layer IV (Wong-Riley, 1979; Spatz et al., 1994). A further comparison of sections demonstrated that the MHC I protein was expressed in neurons in layer IV, which is the cortical layer receiving the majority of projections from the thalamic relay center, the LGN.

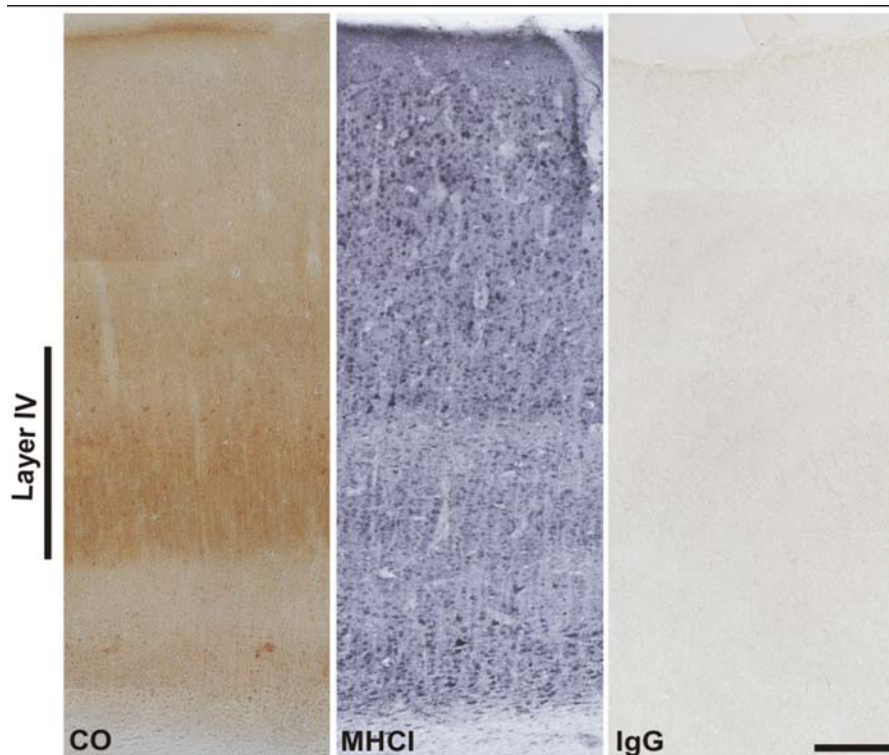


**Figure 10. MHC class I immunoreactivity and cytochrome oxidase (CO) activity in the visual cortex of the common marmoset.** Coronal sections of the marmoset visual cortex probed with TP25.99 antibody revealed strong staining of neurons in all layers (middle image) in animals of all ages. An adjacent section was probed for CO activity (left image), which specifically stains layer IV neurons throughout the visual cortex. Control mouse IgG showed no reaction (right image). Scale bar: 200  $\mu$ m.

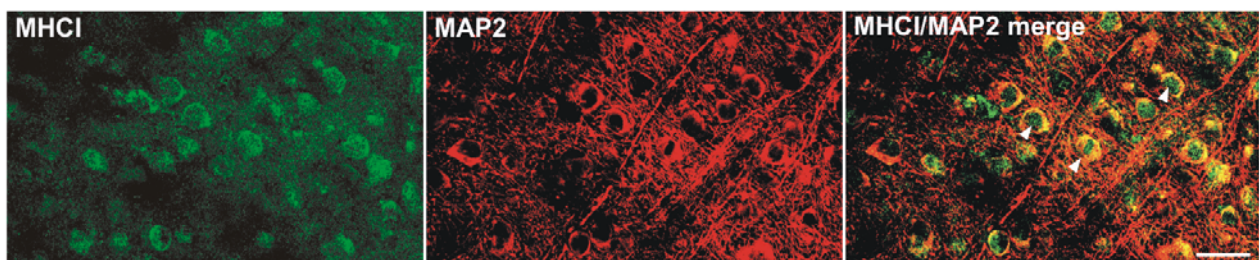


**Figure 11. MHC class I protein colocalizes with the neuronal marker MAP-2 in layer IV neurons of the visual cortex.** MHC class I (green) is localized mainly to neuronal somata, and staining overlaps with that of MAP-2 (red) signal. Sites of colocalization appear in yellow (right picture; white arrowheads). Scale bar: 25  $\mu$ m.

To investigate whether MHCI protein expression is neuronal, double-labeling experiments were performed using TP25.99 and microtubule associated protein 2 (MAP2) which is an established neuronal marker. A punctate pattern of MHCI immunoreactivity that colocalized with MAP2 was observed primarily throughout the neuronal somata of layer IV neurons (Figure 11). Furthermore, additional double labeling experiments using TP25.99, gephyrin and SAP102 (synapse-associated protein of 102 kDa) demonstrated that there was no difference in localization of MHCI protein between excitatory and inhibitory neurons and synapses. Gephyrin is a postsynaptic component of inhibitory synapses (Kirsch and Betz, 1993), while SAP102 is a marker of excitatory synapses (Müller et al., 1996). MHCI protein partially colocalizes with both proteins, but there is no significant difference in the degree of colocalization (Figure 12).

A high level of MHCI immunoreactivity was also present in the subcortical white matter of the occipital lobes. This region contains specialized glial cells, the radial glia, involved in neuronal development and migration (Campbell and Götz, 2002). Radial glia in the primates are distinguished from other types of glial cells (such as astrocytes) by their long processes, as well as by being positive for expression of vimentin, a member of the intermediate filament protein family (Lazzari and Franceschini, 2001; Campbell and Götz, 2002). The MHCI immunofluorescent signal highly overlaps with that of vimentin in the subcortical region of the occipital lobes (Figure 13), indicating its presence on radial glial cells. In addition, almost no overlap is observed between signals of MHCI and the astrocyte marker GFAP in the cortex, further proving that MHCI is specifically expressed by neurons in the visual cortex (Figure 13).

### Layer IV visual cortex

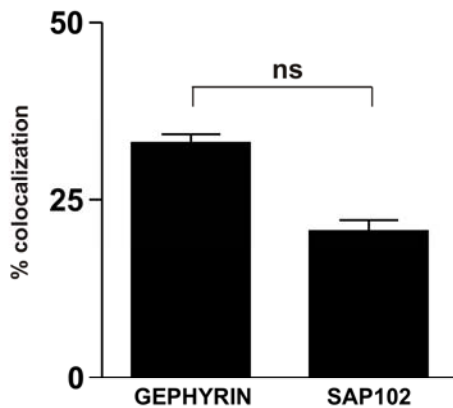
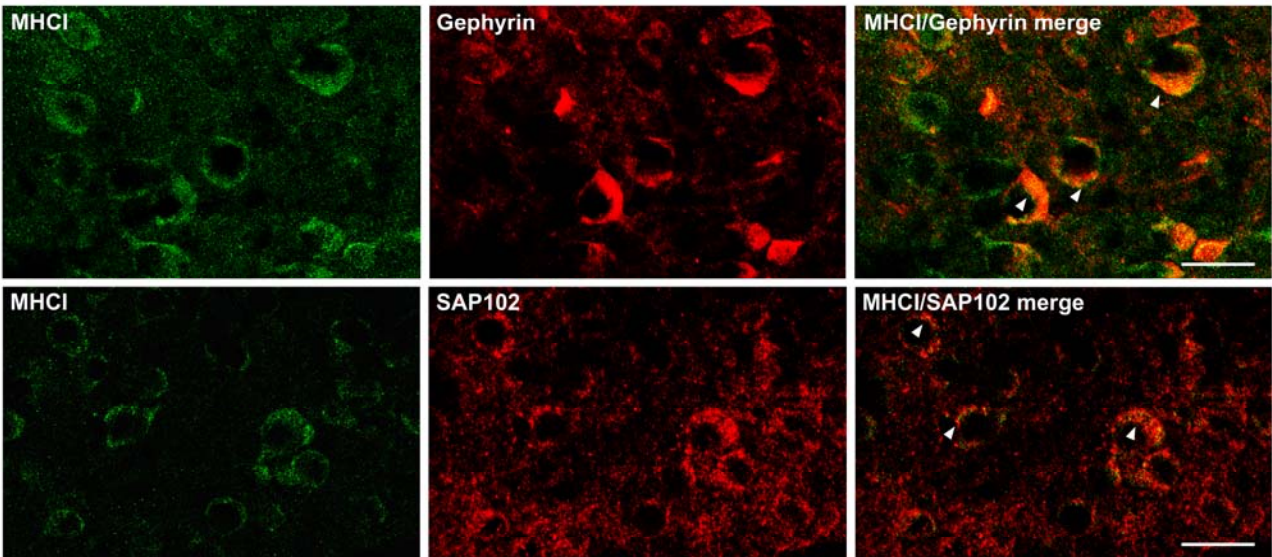


**Figure 12. MHC class I protein is localized to both inhibitory and excitatory neurons in the visual cortex.** Upper row: MHC class I (MHC I, green) partially colocalizes with inhibitory synapse marker gephyrin (red). Lower row: MHC class I (green) partially colocalizes with the excitatory synapse marker SAP102 (red). Points of colocalization are marked by white arrowheads in merged images. There was no significant difference with respect to colocalization of MHC class I with the two synaptic markers (graph). Data are expressed as mean $\pm$ SEM (standard error of the mean), n = 3/group. Scale bar for all images: 20  $\mu$ m.

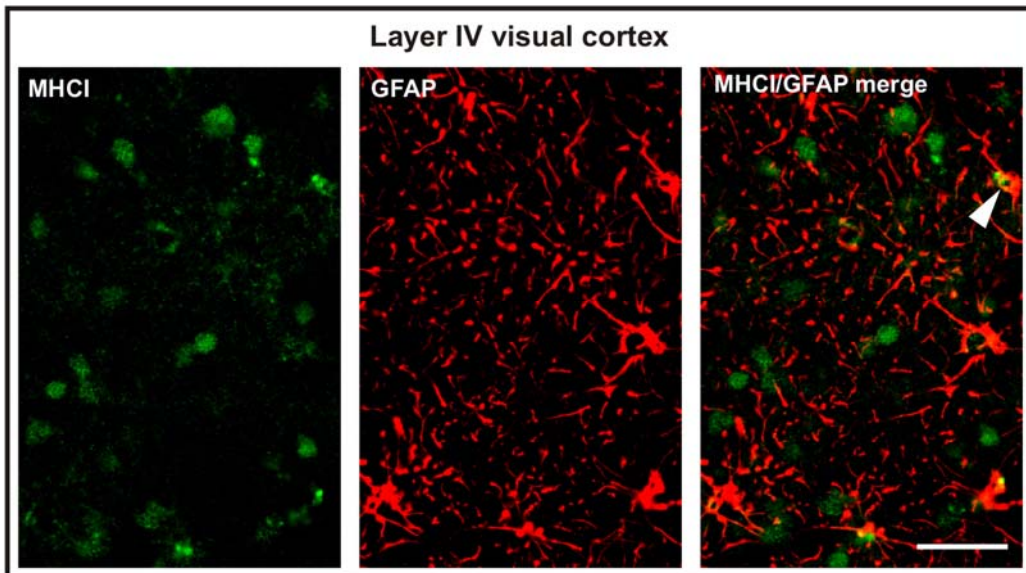
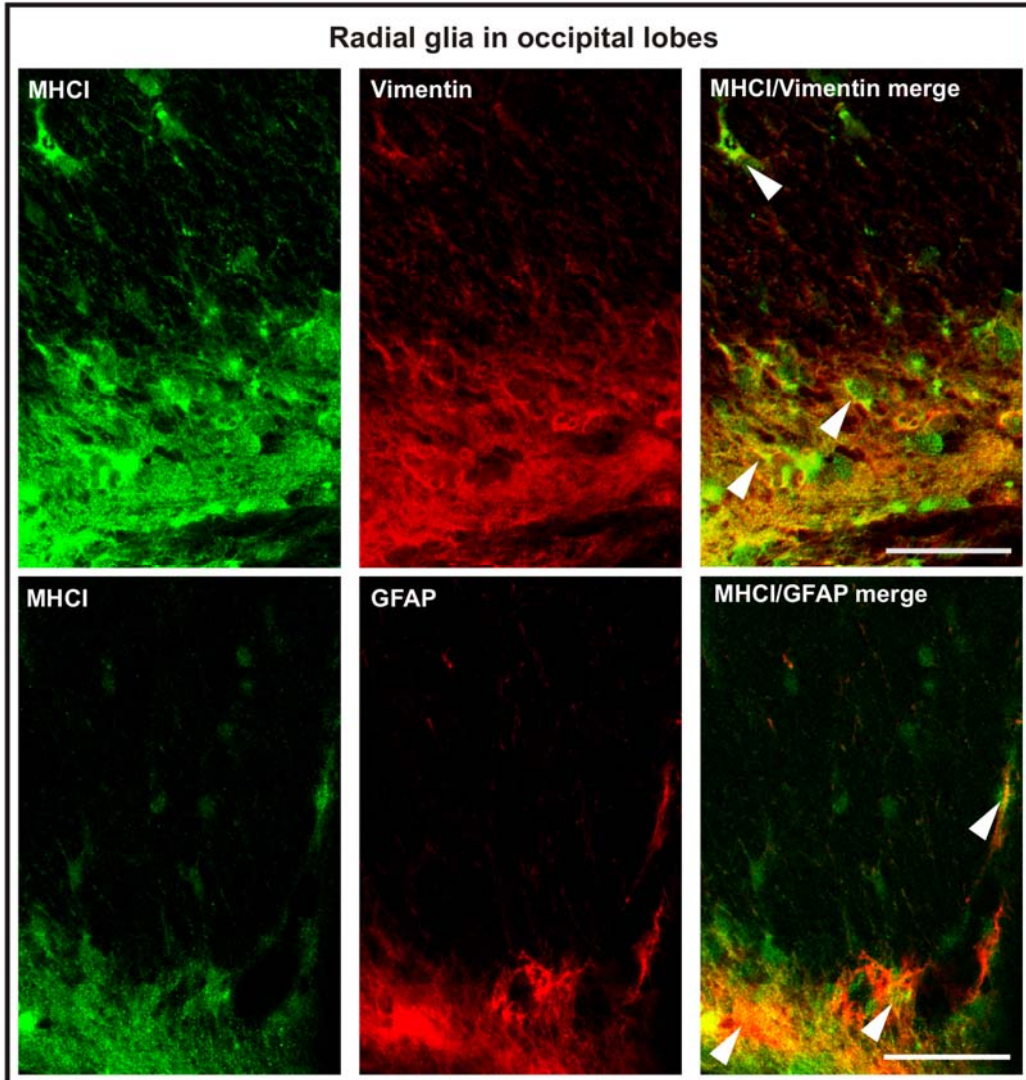


Figure 13. MHC class I protein is localized on radial glial cells in occipital lobes.

**Figure 13 continued.** In the occipital lobes, MHC class I (green) is localized to radial glial cells (red) that are both vimentin and GFAP positive in that region. In the layer IV of the visual cortex, MHC class I signal (green) is rarely found overlapping with GFAP-positive astrocytes (red). Points of colocalization are marked by white arrowheads in merged images. Scale bar for all images: 15  $\mu\text{m}$ .

### **3.1.2. MHC class I expression levels are regulated by neuronal activity**

Several studies have suggested a variety of non-immune roles for MHCI molecules, most of which refer to receptor trafficking and cell growth and differentiation (Fishman et al., 2004). As the temporal and spatial pattern of MHCI expression correlates with synaptogenesis in the visual cortex, this aspect was further studied in the present thesis. The ocular dominance shift is a synaptic phenomenon that is induced by deprivation of visual input from one eye. Enucleation of one eye before critical stages of development changes the pattern of synapses of neurons in V1, because the groups of neurons receiving input from the intact eye increase both the number of their synapses and their strength at the expense of the target neurons of the enucleated eye (Berardi et al., 2003; Sur and Rubenstein, 2005). It is known that the synaptic input regulates gene expression in target neurons and previous gene expression studies have reported major activity-dependent changes in the expression of numerous genes (Lachance and Chaudhuri, 2004; Tropea et al., 2006). Anatomical changes after long periods of deprivation from visual input were also observed, which suggests that the V1 region that receives the input from the intact eye grows at the expense of the region subserving the deprived eye (Hubel et al., 1977). Monocular enucleation (ME, complete removal of one eye) was used to induce an ocular dominance shift in V1 of the marmoset brain. Animals were enucleated at one month of age and were sacrificed at five months of age as described before (DeBruyn and Casagrande,

1981). Expression of MHC I genes between visual cortices of monocularly enucleated animals and age-matched control animals was compared using qRT-PCR with pan-specific MHC I PCR primers. Interestingly, monocular enucleation upregulated expression of MHC I transcripts (Figure 14). Quantitative *in situ* hybridization using the Caja-G probe confirmed the qRT-PCR results revealing a higher density of silver grains on cells in the visual cortex of the enucleated animals (Figure 15).

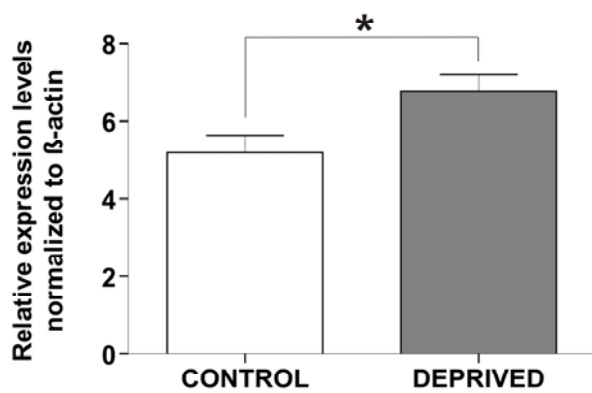


**Figure 14. MHC class I mRNA expression levels are upregulated in response to monocular enucleation.** qRT-PCR revealed significant differences in MHC class I (MHC I) mRNA expression levels between visual cortices of animals that have undergone monocular enucleation (deprived) and control animals. Data are expressed as mean $\pm$ SEM (standard error of the mean), n = 3/group. Significant differences between groups as determined by Student's *t*-test: \*,  $p < 0.05$ .

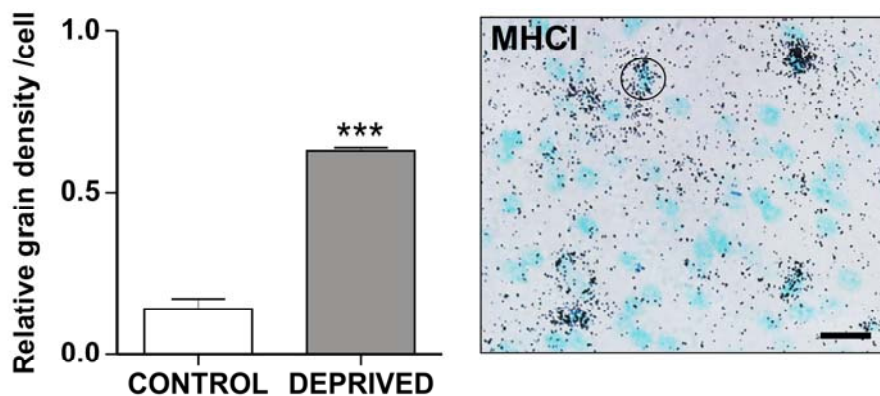


**Figure 15. Quantitative *in situ* hybridization of MHC class I mRNA.** Numbers of silver grains per cell reveal elevated levels of MHC class I expression in the visual cortex of enucleated animals. Example of sections from layer IV of the visual cortex showing silver grains over cells (circular counting mask). Section was counterstained with methylgreen (cyan). Data are expressed as mean $\pm$ SEM (standard error of the mean). Significant differences between groups as determined by Student's *t*-test: \*\*\*,  $p < 0.001$ . Scale bar: 20  $\mu$ m.

### **3.1.3. Neurons expressing higher levels of MHC class I are innervated by afferents from the intact eye**

To further localize MHCI expression in the V1 of the enucleated animals, immunohistochemistry using the TP25.99 antibody was performed, which revealed a patchy pattern of immunoreactivity in layer IV of enucleated animals (Figure 16, A). The optical density profile of MHCI staining across layer IV of the enucleated animals displayed variations in intensity that were not observed in control animals (Figure 16, E). Regions with high and low immunoreactivity, which probably corresponded to ODCs, were detected in these animals. The staining fluctuations observed in the enucleated animals seemed most pronounced in layer IV. In contrast, control animals displayed a relatively uniform staining of layer IV (Figure 16, B).

To assign the regions of high and low immunoreactivity in the enucleated animals to neurons innervated by the intact or the enucleated eye afferents, adjacent sections stained for MHCI and activity marker c-Fos were compared. Expression of c-Fos was uniform, albeit at a really low level in control animals (Figure 16, D); however, in animals that have undergone monocular enucleation, patches of c-Fos immunoreactivity are visible throughout upper parts of layer IV (Figure 16, C). This was consistent with previous studies which demonstrated that levels of c-Fos expression are activity dependent in the visual cortex (Soares et al., 2005; Van der et al., 2007). Comparison of adjacent sections stained for MHCI and c-Fos demonstrated that regions with high MHCI immunoreactivity overlap with regions of high c-Fos immunoreactivity (Figure 16, A and C). Furthermore, the width of columns exhibiting high and low MHCI immunoreactivity was measured, as it was previously shown that columns receiving afferents from the intact eye are wider and occupy larger

regions in the V1 (Fonta et al., 2000). The images of MHCI staining were contrast enhanced and the boundaries of columns were determined using light microscopy. A significant difference was found between the widths of columns exhibiting high and low immunoreactivity, with stronger MHCI staining intensity being localized in the wider columns (Figure 17). These results confirmed the hypothesis that the columns with higher MHCI immunoreactivity receive afferents from the intact eye, which suggests that high expression levels of this gene are associated with higher neuronal activity.

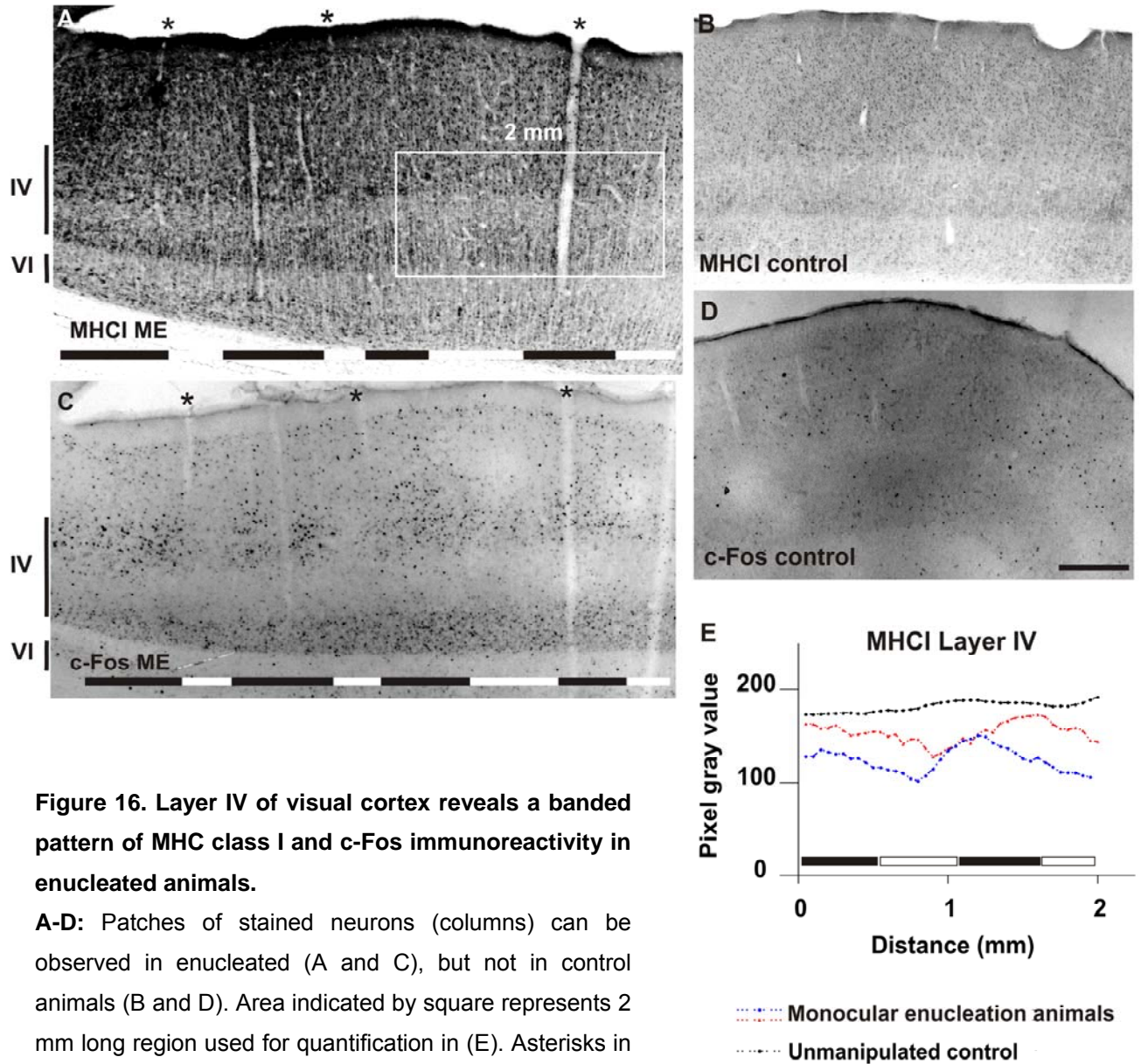


**Figure 16. Layer IV of visual cortex reveals a banded pattern of MHC class I and c-Fos immunoreactivity in enucleated animals.**

**A-D:** Patches of stained neurons (columns) can be observed in enucleated (A and C), but not in control animals (B and D). Area indicated by square represents 2 mm long region used for quantification in (E). Asterisks in A and C denote identical blood vessels. Optical profile

was measured throughout layer IV (indicated by line on the left side of the images). Scale bar for C and D (in D): 0.5 mm)

**E:** Diagram showing the optical density profiles recorded from layer IV (indicated by lines on the left side photographs) in a control animal (black dotted line) and two enucleated animals (red and blue dotted lines).

**Note:** In both photographs and in the diagram black lines indicate areas with high MHC class I and c-Fos immunoreactivity, while white lines point to low immunoreactivity areas.

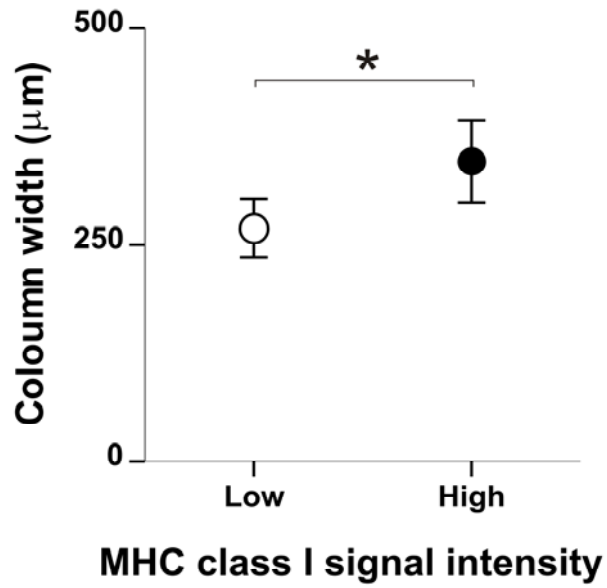


**Figure 17. Neurons exhibiting higher MHC class I levels are receiving afferents from the intact eye.**

Width of MHC class I immunoreactive columns showing that the wider columns display stronger MHC class I staining, which indicates that MHC class I levels are elevated in neurons receiving afferents from the intact eye. Significant differences between groups as determined by Student's *t*-test: \*,  $p < 0.05$ . Data are expressed as mean  $\pm$  SEM (standard error of the mean),  $n = 3$  animals, 10 measurements per animal.

## **3.2. Part II: the hippocampus**

### **3.2.1. Expression of MHC class I molecules in the hippocampus of the common marmoset**

To investigate the expression of MHCI genes in the marmoset hippocampus, a full length clone of the classical marmoset MHCI gene, Caja-G, was also used for *in situ* hybridization experiments. Strong MHCI signals were detected throughout the brain, with particularly strong expression in the hippocampus (Figure 18). The MHCI signal is present in all hippocampal subregions with particularly strong expression in the dentate gyrus and the CA3 subfield (Figure 18, A). Emulsion autoradiography revealed silver grains clustered over granule cells of the dentate gyrus (Figure 19, E) and in the CA3 pyramidal cells region (Figure 18, C). Expression of MHCI was present in all ages examined with little variation in intensity. The sense probe, used as control, revealed no signal which demonstrated the specificity of the MHCI probe (Figure 18, B, D and G).

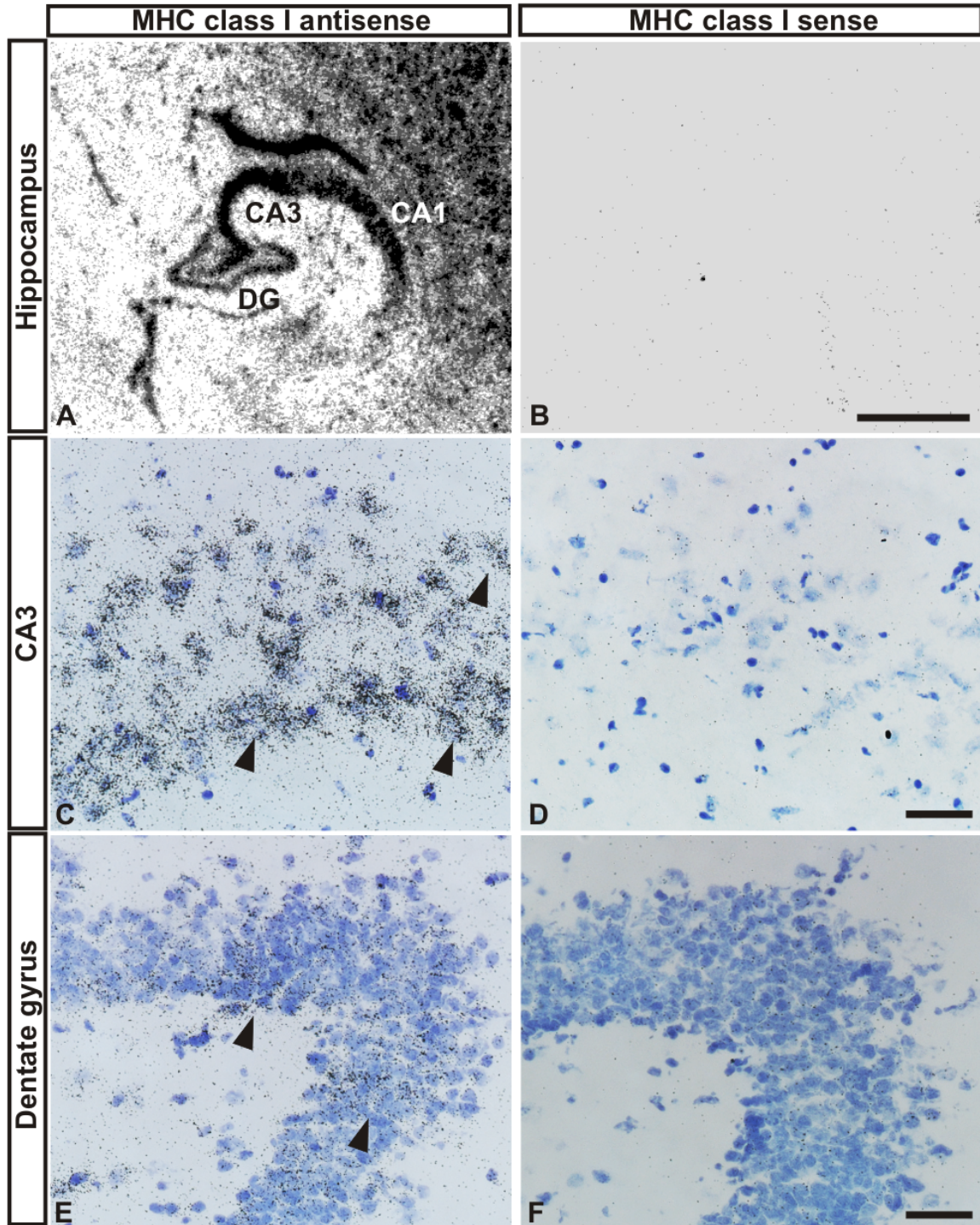


**Figure 18. MHC class I genes are strongly expressed in the marmoset hippocampus.** The labeled MHC I riboprobe revealed strong signals throughout the hippocampal formation, especially in the dentate gyrus and the CA3 subfield (A). Emulsion autoradiography revealed silver grains clustered over cells in the CA3 region (C) and over cells in the dentate gyrus (E).

**Figure 18 continued.** Lack of signals with the sense probe (B, D and F) confirmed specificity of the *in situ* hybridization. Abbreviations: CA1 Cornu Ammonis 1, CA3 Cornu Ammonis 3, DG dentate gyrus. Scale bar for A and B: 1mm. Scale bars for C-F: 10  $\mu$ m.

As previously mentioned, specific antibodies against marmoset MHCI proteins are not available; however, their high similarity with the human homologues allowed us to use the well-characterized HCA2 and HC10 antibodies against human MHCI proteins for the detection of the marmoset MHCI proteins (Stam et al., 1990). These antibodies were used since TP25.99 antibody (used in detection of MHCI proteins in the visual cortex), gave only weak signals in both Western blots of hippocampal proteins and immunocytochemistry performed on hippocampal brain sections. On the other hand, Western blot analysis with HCA2 and HC10 revealed that both antibodies recognized a clear band of approximately 45 kDa, which is the expected molecular weight of the MHCI heavy chain (Figure 19, A). Immunocytochemistry using the HCA2 antibody (Figure 19, B and F) exhibited a striking similarity with the Timm's stain, which specifically stains mossy fibers in the hippocampus (Figure 19, D and H; Henze et al., 2000).

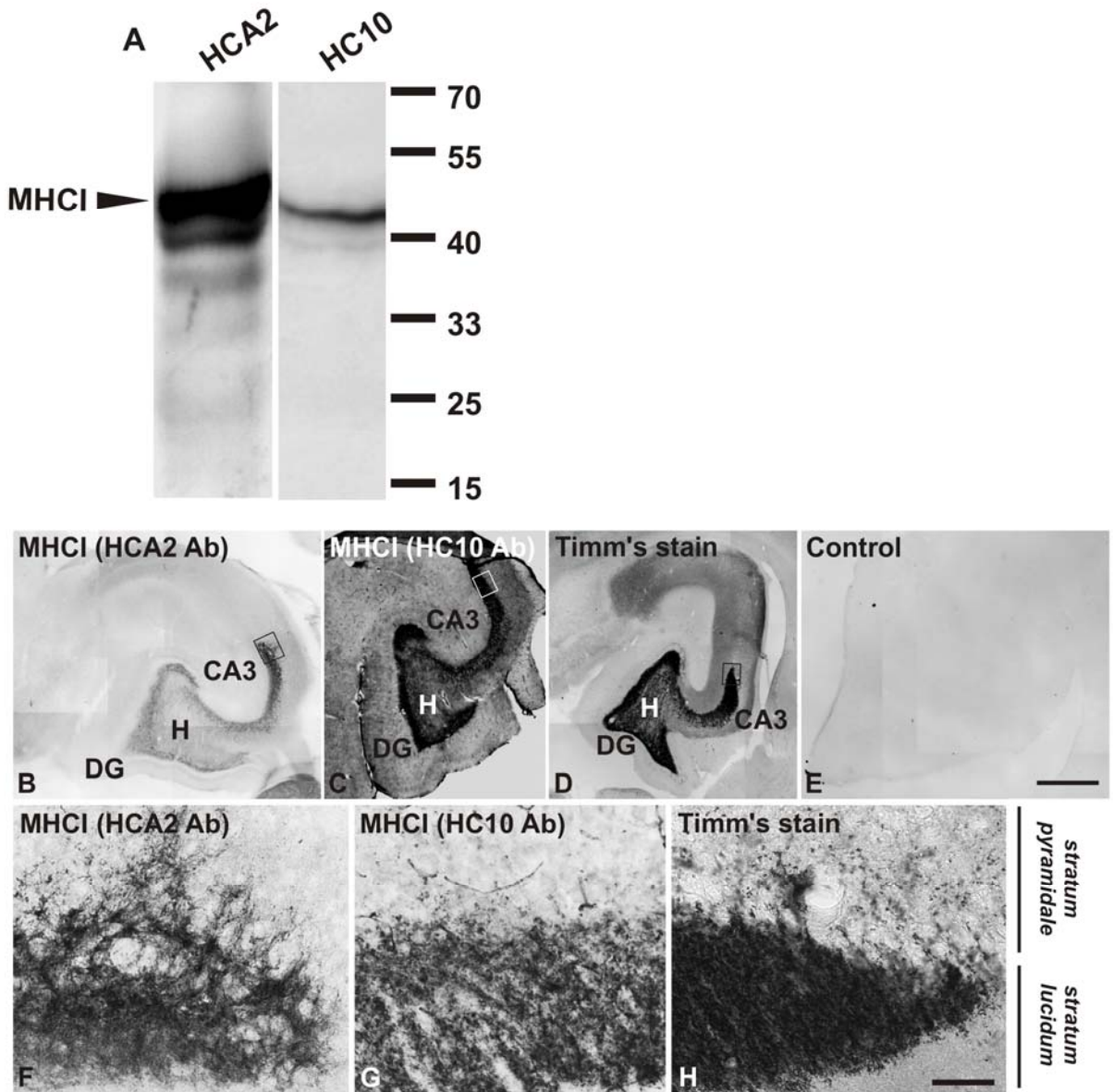


**Figure 19. MHC class I protein is expressed in the mossy fiber pathway.** (A) HCA2 and HC10 antibodies recognized bands matching the reported molecular weight of MHC class I (MHCI) heavy chain (45 kDa) in Western blots of protein extracts from marmoset hippocampi. Protein marker molecular weights are indicated in kDa. **Half-tone photographs:** Both antibodies against MHCI proteins, HC10 and HCA2, gave almost identical staining pattern (B, C, F and G) with intense labeling throughout the stratum lucidum. Staining was very similar to the Timm's stain (D and H) which specifically labels the mossy fiber pathway. Control antibody revealed no staining (E). Abbreviations: Ab antibody, CA3 Cornu Ammonis 3, DG dentate gyrus, H hilus. Scale bar for A-D: 1mm. Scale bars for E-G: 50  $\mu$ m.

The strongest immunostaining was present in the stratum lucidum (Figure 19, B). The HC10 antibody displayed an almost identical staining pattern (Figure 19, C and G); however, blood vessels were also stained with this antibody. Therefore, HCA2 antibody was exclusively used in further double-labeling experiments. It is important to note that no staining of neuronal somata could be detected using these antibodies, even after the epitope retrieval step. MHCI signal was detected solely within mossy fibers in the hippocampal formation. These antibodies did not stain the CA1 and CA2 areas.

### **3.2.2. A subset of MHC class I proteins is localized on the presynaptic side of the mossy fiber-CA3 synapse**

MHCI molecules in the hippocampus of mice have been reported to localize exclusively to the postsynaptic side (Goddard et al., 2007) which is not in accordance with the mossy fibers expression observed in this study. To investigate the synaptic localization of MHCI, double-labeling experiments were performed using MHCI, piccolo [a marker of the presynaptic active zone (Cases-Langhoff et al., 2000)], and SAP102 [synapse-associated protein of 102 kDa, marker of postsynaptic densities (Müller et al., 1996)]. Quantification of immunofluorescence revealed that clusters of MHCI signals overlapped with piccolo signals (Figure 20, A and C), whereas no overlap was detected with SAP102 (Figure 20, B). These data suggest that MHCI is localized to the presynaptic side.

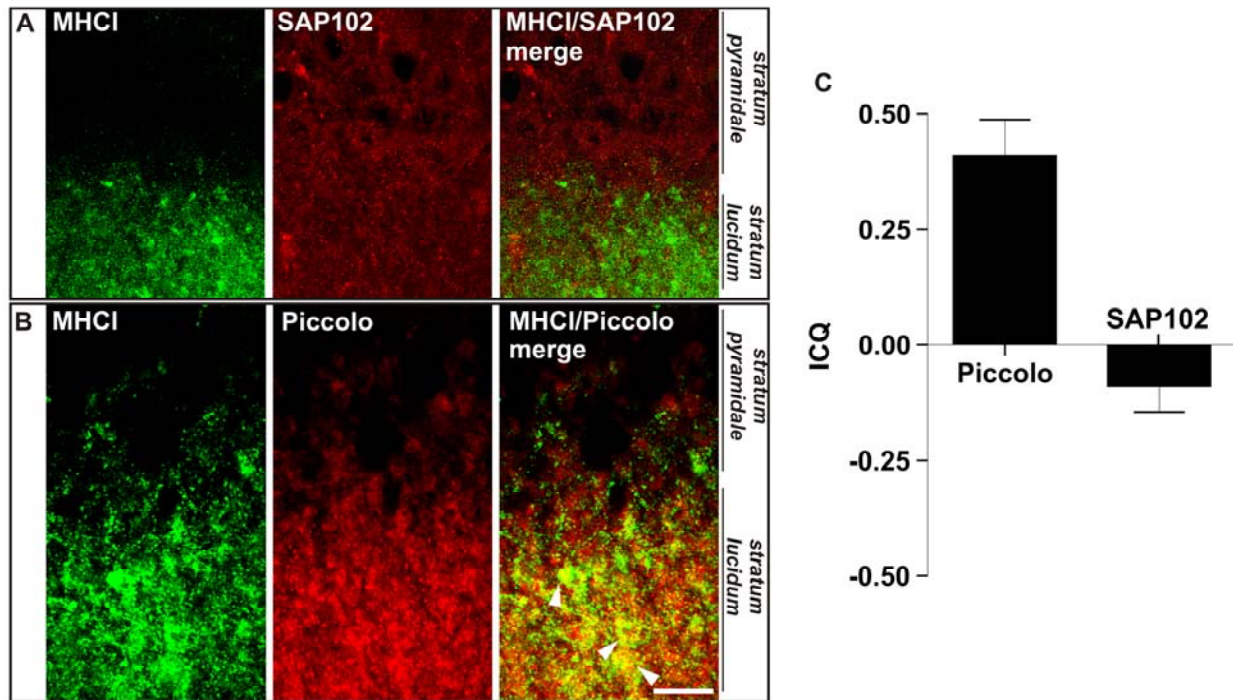


**Figure 20. MHC class I (MHCI) protein is localized to the presynaptic side of the mossy fiber-CA3 synapse.** MHCI signal (green) significantly overlaps with that of piccolo (red), a marker of the presynaptic active zone (A, white arrowheads). Almost no overlap is detected between MHCI and the postsynaptic marker SAP102 (B). Quantification of immunofluorescence revealed that MHCI is associated with the presynaptic side of the mossy fiber-CA3 synapses (C). Data shown represent means  $\pm$  SEM, N=3. Scale bar for A and B: 30  $\mu$ m.

### 3.2.3. MHC class I proteins are present on the giant mossy fiber terminals

Hippocampal mossy fibers represent projections from granule cells of the dentate gyrus to the hilar mossy cells and to the CA3 pyramidal neurons of the hippocampus (Henze et al., 200; Nicoll and Schmitz, 2005). The terminals of mossy fibers form specialized “giant” terminals that innervate the apical dendrites of the CA3 pyramidal neurons. Small terminals innervate the interneurons present in the hilus and in the stratum lucidum (Henze et al., 2003; Nicoll and Schmitz, 2005). The vesicular glutamate transporter 1 (VGlut1) mainly localizes to the large mossy-fiber terminals (Bellocchio et al., 1998; Herzog et al., 2001)

whereas the vesicular glutamate transporter 2 (VGlut2) is present in small terminals, which contact the inhibitory interneurons and are VGlut1 negative (Herzog et al., 2001). To characterize the localization of MHC I protein in mossy fibers further, its colocalization with VGlut1 and VGlut2 was assessed. MHC I proteins predominantly colocalized with VGlut1-immunopositive clusters, where the two immunofluorescent signals intensively overlapped (Figure 21, A and C). Very little colocalization was observed with VGlut2 signals (Figure 21, B) which suggests that the MHC I protein mainly localized to the large mossy fiber terminals that innervate CA3 pyramidal neurons.

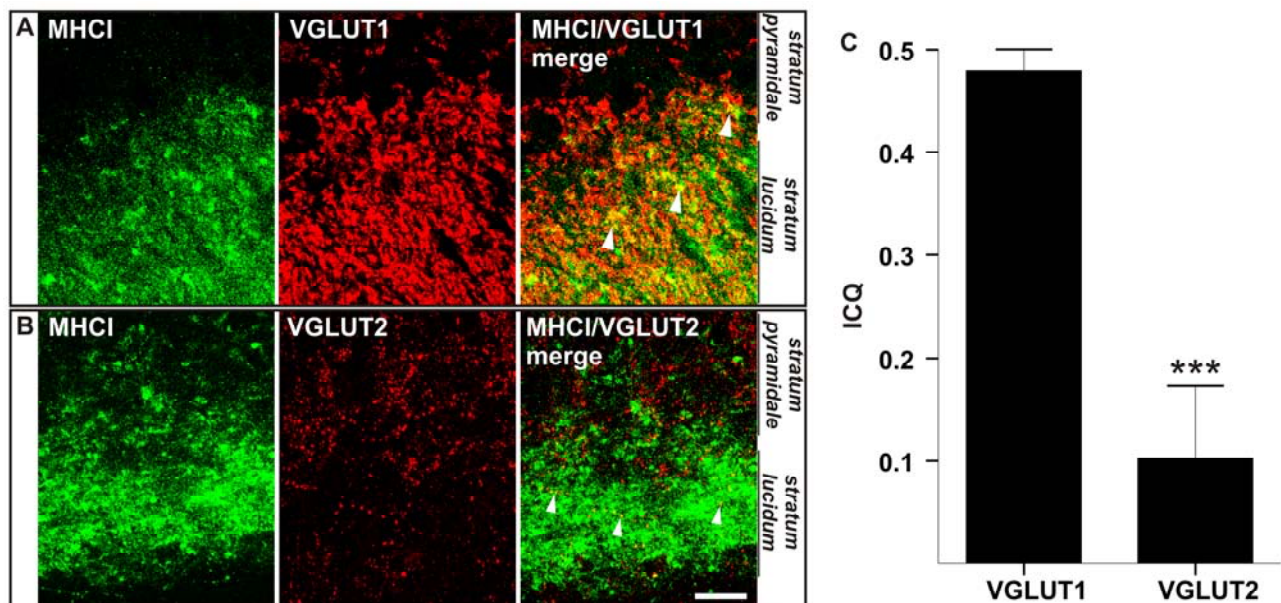


**Figure 21. MHC class I (MHC I) protein is present on large mossy fiber boutons.** MHC I is predominantly localized on VGlut1 positive large mossy fiber boutons (A, white arrowheads) while very little overlap is seen between MHC I and VGlut2, which labels small mossy fiber boutons and filopodial extensions (B). Quantitative immunofluorescence revealed a significant difference between MHC I signals overlapping with VGlut1 and VGlut2, respectively (C). Data represent means  $\pm$  SEM, N=3 animals. Significant differences between groups as determined by Student's *t*-test: \*\*\*,  $p < 0.001$ . Scale bar for B and C: 30  $\mu$ m.

### 3.2.4. Neuronal MHC class I proteins are involved in excitatory transmission at mossy-fiber CA3 synapses in the marmoset hippocampus

To elucidate potential functions of the neuronal MHCI proteins, whole-cell patch-clamp recordings of CA3 neurons in acute slices of the marmoset hippocampus were performed. As the gene knockdown technology in primates is still in its early stages, cell-surface expression of MHCI proteins was interfered with via the application of HCA2 and HC10 antibodies. Although HC10 and HCA2 were raised against denatured MHCI heavy chains, they specifically immunoprecipitated native marmoset MHCI from cells transfected with a tagged marmoset MHCI (Figure 22) using both antibodies.

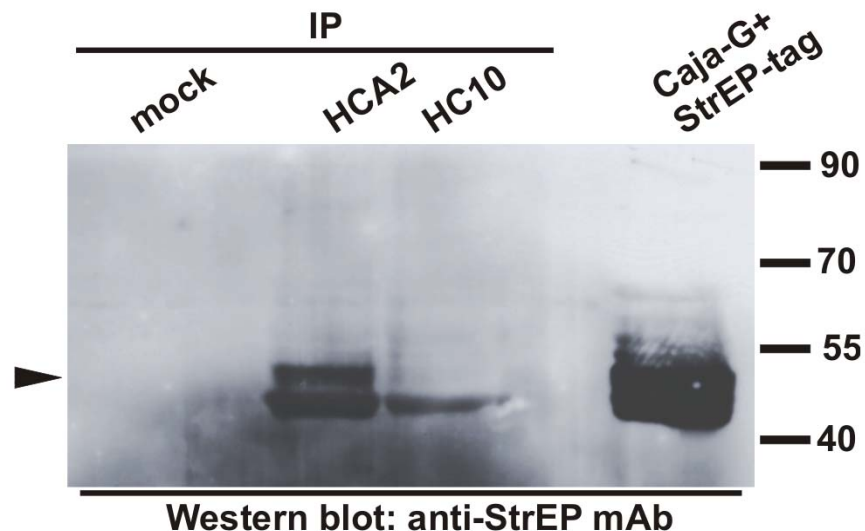


**Figure 22. HCA2 and HC10 recognize native marmoset MHC class I (MHCI) protein.** HEK293T cells were transfected with the marmoset MHCI construct carrying StrEP-tag. Protein extracts were immunoprecipitated with HCA2 and HC10 antibodies under non-denaturing conditions and analyzed by Western blotting with an antibody against the StrEP-tag. Both antibodies, HCA2 and HC10, precipitated the StrEP-tagged marmoset MHCI; mock (beads only) revealed no signals. Purified marmoset MHCI with StrEP-tag (Caja-G+StrEP-tag) was used as a positive control. Protein marker molecular weights are indicated in kDa (numbers on the right side).

As MHCI proteins were localized almost exclusively to the mossy-fiber terminals in the marmoset hippocampus, we investigated the changes in spontaneous excitatory postsynaptic potentials (sEPSCs) solely in CA3 neurons were investigated. Application of HC10 and HCA2 antibodies significantly decreased the frequency of sEPSCs (Fig. 24). The normalized mean frequency of sEPSCs decreased by 28.75% ( $\pm$  10.28%) 5 min after the application of the antibodies compared with the baseline level (100%). Twenty minutes after the application of the antibodies, the normalized mean frequency decreased by 39.23% ( $\pm$  9.27%) [Figure 23, A (right panel) and B]. In addition, application of these antibodies also transiently increased the normalized amplitude of the sEPSCs by 22.4% ( $\pm$  10.62%) after 10 min (Figure 23, A and C). Application of the control IgG had no significant effect on the frequency or the amplitude of sEPSCs [Figure 23, A (left panel), B, and C]. These data suggest that MHCI proteins have a specific function in neurotransmission at the mossy-fiber CA3 synapse.

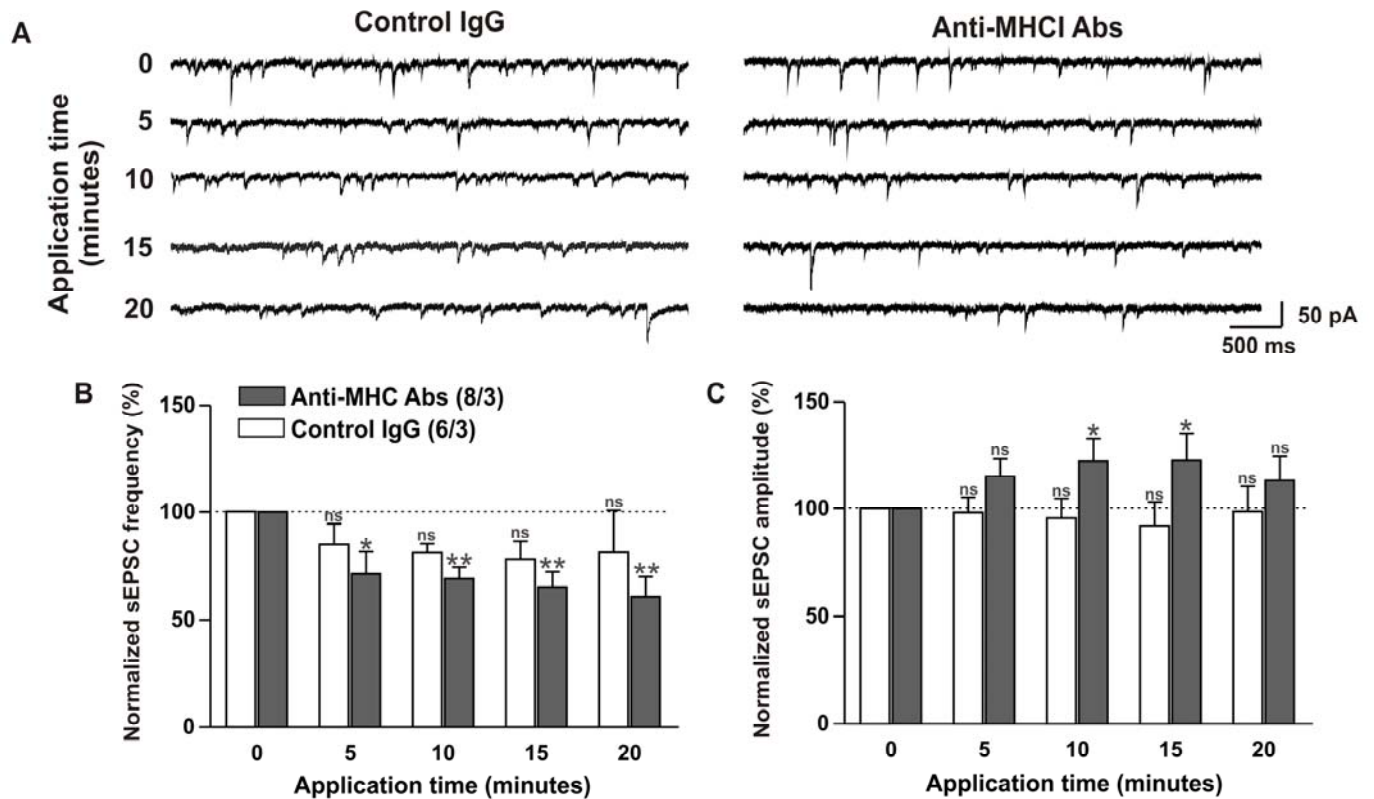


**Figure 23. Application of antibodies against MHC class I (MHCI) proteins to marmoset hippocampal slices decreases the frequency of sEPSCs.** (A) Representative recordings of spontaneous pharmacologically isolated excitatory postsynaptic currents (sEPSC) from CA3 neurons during the experiment. Recordings with the application of control immunoglobulins are on the left side, and recordings with the application of antibodies against MHCI proteins are on the right side. (B) Averaged frequency of spontaneous EPSCs significantly decreased after 10 minutes of antibody application. Normalized mean frequency of sEPSCs decreased 28.75 % (+/- 10.28) five minutes after the application of the antibodies and continued to decrease down to 39.23 % (+/- 9.270) of baseline level (Figure 4, A (right panel), B). In addition, application of antibodies also transiently increased the normalized amplitude of sEPSCs by 22.4 % (+/- 10.62) compared to baseline level after 10 minutes (Figure 4, A, C). Application of control IgG had no significant effect on either the frequency or the amplitude of sEPSCs. Data represent means  $\pm$  SEM. Numbers within the graphs indicate the number of neurons/animals tested for each experimental group. Distribution of data was tested with the Kolmogorov–Smirnov test. Significant differences between groups as determined by One-way ANOVA with repeated measures and Dunnett’s post hoc-test using measurements taken within the first three minutes of recording as control: \*,  $p < 0.05$ , \*\*,  $p < 0.01$ .

## 4. Discussion

Several recent studies have implicated MHCI proteins in the proper development of connectivity in the central nervous system (Corriveau et al., 1998; Huh et al., 2000; Goddard et al., 2007). These molecules have been shown to play an important role in synaptic refinement in mice, where they are involved in the weakening and removal of excess synapses formed during normal development of the visual system (Huh et al., 2000). Moreover, they are required for induction and maintenance of long term depression in the hippocampus of mice (Huh et al., 2000). Because of the differences between rodents and primates in the organization of the CNS and in the MHCI gene family structure, the expression of neuronal MHCI in the primate brain was investigated in the present thesis.

### 4.1. Cellular localization of MHC class I molecules in the visual cortex

It is known that virtually all nucleated cells express MHCI genes; however, the visual cortex MHCI proteins are primarily expressed on neurons, and not on astroglial cells. Double-labeling experiments clearly showed that MHCI proteins are expressed on MAP2 positive neurons, although no differences were detected with regard to MHCI localization on inhibitory vs excitatory neurons. *In situ* hybridization and immunohistochemistry revealed high expression levels of MHCI throughout the subcortical white matter of the occipital lobes. MHCI protein colocalized with vimentin-positive radial glia cells in that region. However, GFAP-positive glial cells (astrocytes) throughout the visual cortex were largely negative for MHCI protein expression. The presence of MHCI proteins on radial glial cells even further implicates MHCI in the proper development of the visual cortex, since these

highly specialized cells are hypothesized neuronal precursors and are involved in proper development and migration of cortical neurons (Campbell and Götz, 2002).

#### **4.2. MHC class I in the developing visual system**

In contrast to previous studies in rodents and cats (Corriveau et al., 1998; Huh et al., 2000), expression of MHCI in the LGN at postnatal stages was not detected here. It is possible that MHCI genes are expressed prenatally in the marmoset LGN, as segregation of LGN layers in primates occurs *in utero* (Rakic, 1976 and 1977). Furthermore, the probe used here for detection of the MHCI transcripts is specific for a smaller subset of MHCI molecules, while the probes used in previous studies were pan-specific and therefore detected a larger variety of MHCI molecules (Corriveau et al., 1998). Nonetheless, the present data showed that MHCI genes were strongly expressed throughout the visual cortex of the marmoset. At early postnatal stages (between days 1 and 7), expression was primarily concentrated in layers I and IV. But in older animals, the expression pattern became diffuse and widespread throughout all neuronal layers. Extremely strong expression levels were present in the subcortical white matter in young animals, but this signal declined with advancing age.

The levels of expression of MHCI protein in the visual cortex correlated with the levels of SNAP-25, and the expression of both proteins was found to be highest during the third postnatal month. SNAP-25 is an established synaptogenesis marker (Oyler et al., 1991; Gingras et al., 1999) and previous findings that synapse density in the marmoset visual cortex reaches very high values in the third postnatal month were confirmed here (Missler et al., 1992 and 1993). After postnatal month three, mainly during the fifth postnatal month,

SNAP-25 expression levels in the common marmoset visual cortex are rapidly reduced to adult values. As MHCI genes have been implicated in the removal of excess synapses (Huh et al., 2000), it was expected to find high MHCI expression levels in the fifth postnatal month, at the time when extensive synapse removal occurs in the marmoset visual cortex. However, MHCI protein expression was at its peak in the third postnatal month, similarly to SNAP-25 levels, which suggests that MHCI proteins may exert their action during synaptogenesis rather than during elimination of synapses. The observation that expression of SNAP-25 and MHCI proteins occurs at the same stage of visual cortex development strongly supports the hypothesis that MHCI protein plays a role in synaptogenesis.

#### **4.3. MHC class I expression in the visual cortex is activity dependent**

Because detailed functional studies involving primates are not available, an alternative model to clarify the role of MHCI molecules further in the marmoset visual cortex was used. The ocular dominance shift is a well-known neuroplasticity paradigm that occurs when one eye of the experimental animal has been deprived of visual input during development. Prolonged deprivation (in the order of months) is known to induce morphological changes in the visual cortex, because neurons that receive input from the intact eye expand their territory at the expense of neurons that receive afferents from the deprived eye (Hubel et al., 1977; Shatz and Stryker, 1978). A number of studies addressed gene expression changes after monocular deprivation showing that prolonged monocular deprivation results in the upregulation of growth factors and genes associated with neuronal degeneration, as well as with the upregulation of genes involved in synaptogenesis (Lachance and Chaudhuri, 2004; Tropea et al., 2006; Lyckman et al., 2008). The expression levels of SNAP-25, synaptic

vesicle protein 2b (SV2b), and synaptic cell adhesion molecule (synCAM) are greatly increased during postnatal visual cortex development in mice, which is thereafter followed by a steady decline in expression levels to adult values (Lyckman et al., 2008), similarly to the observations described here for SNAP-25 and MHC I expression levels in the marmoset visual cortex. SNAP-25 and synCAM are required for synaptogenesis (Osen-Sand et al., 1993; Biederer et al., 2002; Sara et al., 2005) and are upregulated in response to monocular deprivation (Lyckman et al., 2008). This indicates their involvement in the development of new neuronal connections, possibly belonging to neurons that receive input from the intact eye, as these cells expand their territory within the visual cortex after deprivation. Interestingly, MHC class I transcript levels were also higher in response to monocular enucleation, indicating a possible role of MHC class I in synaptogenesis (Figure 24).

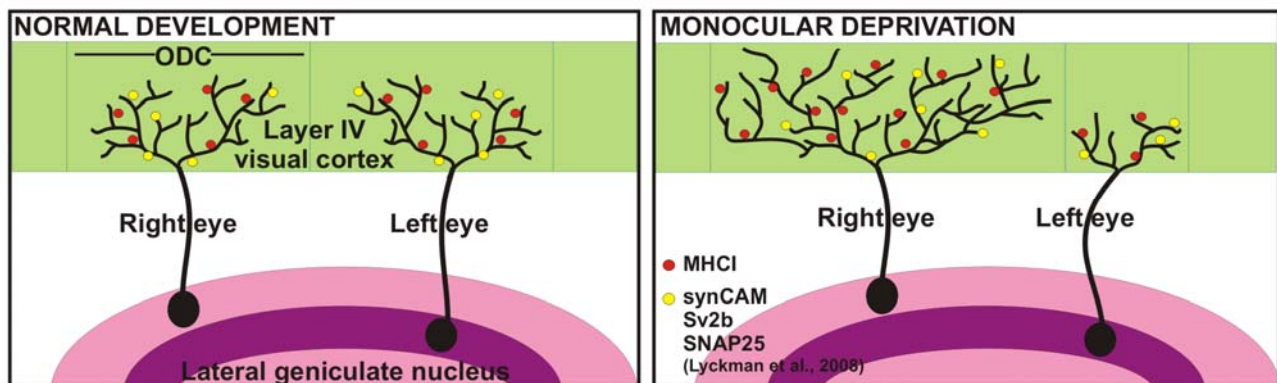


**Figure 24. Schematic representation of effects of monocular deprivation.** In normal development of the visual cortex, various synaptic proteins (yellow dots) along with MHC class I (red dots) are equally **Figure 24 continued.** expressed by neurons receiving afferents from both eyes (left part of the figure). If one eye is deprived of visual input throughout development of the visual system (in the figure: left eye), cortical regions receiving input from the intact eye expand their territory within the visual cortex (in the figure: right eye). This elevates expression levels of proteins required for synaptogenesis, such as synCAM, Sv2b and SNAP25 (Lyckman et al., 2008; right part of the figure). MHC class I levels are also upregulated in regions receiving afferents from the intact eye which points to a possible role of MHC I in synaptogenesis.

Immunohistochemistry was used to localize the elevated MHC class I levels to neurons receiving afferent inputs from the intact eye. Variations in CO staining in enucleated animals were not detected; however, this finding was not surprising, as it has been shown previously that this staining produces different results in different deprivation protocols (Fonta et al., 1997). On the other hand, both c-Fos, a well-established activity marker (Soares et al., 2005; Van der et al., 2007), and MHC class I immunostaining revealed a patchy pattern in layer IV neurons in the visual cortex of enucleated animals. Comparison of adjacent sections stained for both proteins has shown that regions of high c-Fos and MHC class I immunoreactivity overlap. Furthermore, patches with high MHC class I immunoreactivity were wider than the patches with low immunoreactivity. Previous studies in marmosets have shown that such patches correspond to ODCs and that the patches differ in size in monocularly deprived animals with wider ones receiving input from the intact eye (Fonta et al., 2000). Hence, MHC class I immunoreactivity in layer IV of the visual cortex of enucleated animals suggests the upregulation of the expression of this class of genes in neurons receiving input from the intact eye. Taken together, these results point to involvement of MHC class I in synaptogenesis in the primate visual cortex.

The exact mechanism of MHC class I action in the visual cortex is yet to be elucidated, although a couple of possibilities emerge when previous studies on MHC class I are taken into consideration. Studies demonstrating the recruitment of PI-3 kinase by MHC class I molecules (Ramalingam et al., 1997) point to one of the possible mechanisms of MHC class I action, since PI-3 kinase activation is known to induce synaptogenesis (Martin-Pena et al., 2006). Another possibility includes the MHC-presenting peptides, as it is known that they reflect the metabolic state of the cell (Fortier et al., 2008). Given that MHC class I

expression on the neurons of the visual cortex is activity regulated, this would enable it to mark or tag different neuronal populations in, for example, monocular enucleation paradigm: neurons receiving input from the intact eye with enhanced MHC class I expression vs neurons receiving afferents from the enucleated eye with decreased MHC class I expression. In this case, higher MHC class I levels with a specific repertoire of presenting peptides would “tag” the neurons as active, which would entail the stabilization of existing synapses and the development of new ones, and vice versa. Hopefully, future studies and experiments will shed more light on this crucial question.

#### **4.4. Localization of MHC class I molecules in the hippocampus**

Previous results by our group demonstrated a relatively conserved expression pattern of  $\beta$ -2-microglobulin and a subset of MHCI molecules between rodents and primates (Rölleke et al., 2006). However, another subset of MHCI molecules in the common marmoset brain that we investigated in this study revealed a distinct and so far not reported expression pattern and functional properties. Antibodies targeting the heavy chain subunit of MHCI molecules revealed a strong MHCI expression that was confined to the mossy fibers in the hippocampal formation. Both antibodies that we used here are targeting an epitope situated in the most polymorphic part of the MHCI molecules, and are therefore specific for only a small portion of MHCI proteins. Importantly, both antibodies recognized bands of the appropriate sizes in Western blots, and gave almost identical staining patterns in immunocytochemistry which further supports the specificity of the expression. Staining of neuronal cell bodies or dendrites was not detected with these antibodies, although MHCI

mRNA was expressed throughout the CA1-CA3 pyramidal cell layers. Since MHCI molecules encoded by different members of the MHCI gene family are usually highly similar in their nucleotide sequence to one another, a possible explanation for this discrepancy is that the MHCI riboprobe used for *in situ* hybridization studies is cross-hybridizing with another subset of MHCI mRNAs, the products of which are not detected by these two antibodies. This is very likely to be the reason, given that in our previous study MHCI proteins were detected on the soma of CA1-CA3 pyramidal neurons using antibodies raised against the  $\alpha$ -3 domain of MHCI and therefore targeting a larger population of MHCI molecules (Rölleke et al., 2006).

Double labeling experiments indicated that the MHCI protein detected by HCA2 antibody is presynaptic and primarily associated with the large mossy fiber boutons that provide the main excitatory input to the CA3 pyramidal neurons. Thus the present results from marmosets differ from previous findings in mice where MHCI proteins have been found to be localized to postsynaptic sites of hippocampal neurons (Goddard et al., 2007). MHCI proteins have not been detected in the hippocampal mossy fibers of mice, which may be due to a lack of suitable antibodies against mouse MHCI proteins. However, it is also possible that the mossy fiber expression of MHCI is a marmoset (or primate)-specific trait. A subset of MHCI molecules in the marmosets displays expression very similar to the one observed in rodents (Corriveau et al., 1998; Rölleke et al., 2006). Given the high evolution rate of MHCI molecules (Kumanovics et al., 2003), it is likely that a fraction of MHCI developed a new function and localization. A detailed comparative study in rodents and primates with equivalent tools is needed to elucidate this issue.

## **4.5. MHC class I involvement in excitatory transmission at the mossy fiber-CA3 synapse**

As MHCI knockout marmosets or specific neuronal MHCI antagonists are currently not available, antibodies were used here to block MHCI on the surface of mossy-fiber terminals. The normalized mean frequency of sEPSCs was significantly reduced after application of the antibodies and this effect increased proportionally to the duration of the incubation. Furthermore, a small, but significant transient increase in amplitude of sEPSCs was observed. Again, these results did not match the previous observations in rodents, where a lack of surface MHCI expression led to an increase in the mEPSC frequency of hippocampal neurons in MHCI-deficient mice (Goddard et al., 2007). As previously mentioned, it is possible that the MHCI targeted in the present study belongs to a subset of MHCI that was not yet detected in studies in mice due to unavailability of proper tools. However, mice used in the previous studies lacked expression of the majority, if not all, MHCI genes (Goddard et al., 2007). On the other hand, a different recording protocol was used here (spontaneous instead of miniature EPSCs, Goddard et al., 2007) which also may account for some differences in observations.

### **4.5.1. Implications of antibody application in electrophysiological recordings**

Effects observed here are not an artifact of the antibody application since application of control immunoglobulins at the same concentration had no significant effect on synaptic transmission. These results together with previously published data suggest that using

antibodies and peptides to block the cell-surface receptors is a sufficient method for investigating function of proteins for which knock-out models or antagonists are not available (Bufler et al., 1996; Saghatelian et al., 2000; Mameli et al., 2005). On the other hand, it is known that antibodies can cause diverse effects after application to cells in vitro or in their native milieu. With respect to antibodies against MHCI it is known that some antibodies are known to cluster and ligate MHCI molecules on the cell surface which produces various effects (Reed, 2003; Jindra et al., 2008a, 2008b). However, antibodies reported to be used in the majority of experiments are recognizing the fully assembled MHCI comprising of the heavy chain, the presenting peptide and the  $\beta$ -2-microglobulin. HCA2 and HC10 antibodies used in this study detect only a pool of the free heavy chains (FHC) of MHC on the surface of neuronal membranes. Free heavy chains of MHCI are also known as “open conformers” and are found in normal conditions on the cell surface along with the fully assembled MHCI proteins (Arosa et al., 2007). The biological significance of MHCI free heavy chains is not fully clear. They have been implicated in regulation of the T-cell response in the immune system, as well as in regulation of receptor trafficking on cells outside the immune system (Arosa et al., 2007). The best characterized non-immune interaction of MHCI free heavy chains is that with the insulin receptor (IR, Fehlmann et al., 1985; Phillips et al., 1986; Stagsted et al., 1990; Arosa et al., 2007). It has been implied that the free heavy chain of MHCI associates with its polymorphic  $\alpha$ 1 and  $\alpha$ 2 domains with a subunit of IR after insulin binding, thereby affecting subsequent signaling and IR internalization (Stagsted et al., 1990). HC10 and HCA2 bind to epitopes in  $\alpha$ 1 and  $\alpha$ 2 domains of MHCI so we assumed that if these domains are needed for interaction with the yet unknown receptor, application of these antibodies would block that interaction. To

address this in detail, these experiments should be performed again using Fab fragments of HCA2 and HC10.

#### **4.5.2. Potential function of MHC class I molecules in synaptic transmission at the mossy fiber-CA3 synapse**

As previously noted, it is obvious that evolution enabled MHCI molecules with diverse functions, both immune and non-immune (Fishman et al., 2004). A potential explanation for the function of MHCI at the mossy fiber-CA3 synapses arises when previous studies on MHCI and the features of this synapse are taken into consideration. The mossy fiber-CA3 synapse displays a number of peculiarities in comparison to the majority of CNS synapses. It is e.g. characterized by a low basal transmission which is maintained by activation of a number of receptors that have inhibitory effects on synaptic transmission (Nicoll and Schmitz, 2005). Given that the best characterized non-immune function of MHCI is regulation of trafficking and internalization of various receptors (Stagsted et al., 1990; Ramalingam et al., 1997; Arosa et al., 2007), one probable hypothesis for the function of neuronal MHCI consistent with the results obtained here is that MHCI is needed for proper internalization of one or several of those receptors (Figure 25). One may speculate that blocking the interaction of MHCI with such receptors by application of anti-MHCI antibodies would prolong inhibitory signaling thus reducing the frequency of sEPSCs. This does not fully explain the transient increase in the amplitude of sEPSCs; therefore, further electrophysiological analyses are required to dissect the action of MHCI in synaptic

transmission in detail. The identification of interacting partner(s) and signaling mechanisms remain crucial to the elucidation of the function of neuronal MHC I molecules.

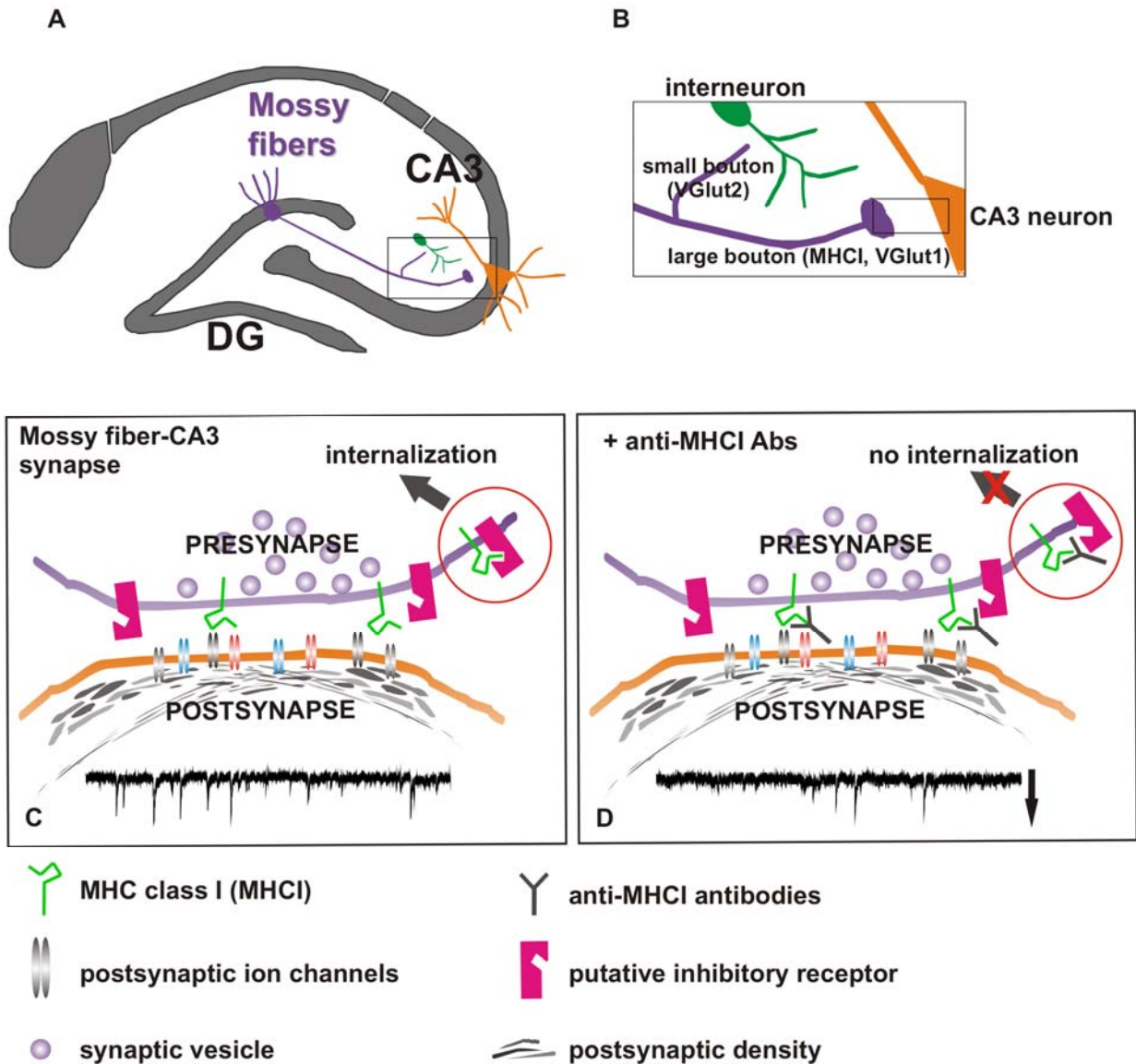


**Figure 25. Schematic representation of potential mode of action of MHC class I at the mossy fiber-CA3 synapse.** (A) Schematic representation of hippocampus. (B) Mossy fibers (purple) terminate on CA3 neurons (orange) in form of large boutons that contain vesicular glutamate transporter 1 (VGlut1) and MHC class I (MHCI). They also terminate on interneurons in the CA3 region (green) in form of small boutons that contain vesicular glutamate transporter 2 (VGlut2). (C) Mossy fiber-CA3 synapse normally displays lower

**Figure 25 continued.** levels of basal activity compared to other synapses in the central nervous system (representative electrophysiological trace of recorded spontaneous EPSCs of a marmoset CA3 neuron is shown in the lower part of the image). This is mainly due to large number of receptors (magenta) that have inhibitory effect on synaptic transmission (Nicoll and Schmitz, 2005). It is possible that MHCI is needed for proper internalization and removal of one of these receptors from the cell surface. MHCI would presumably bind to the receptor with its  $\alpha 1$  and  $\alpha 2$  domains. (D) If anti-MHC antibodies that bind to  $\alpha 1$  and  $\alpha 2$  domains are applied in the vicinity of the cell while the cell's activity is recorded using patch clamp technique, frequency of spontaneous EPSCs is decreased (trace in the lower part of the image). It is possible that antibodies block interaction of MHCI with putative inhibitory receptor, which prolongs inhibitory signaling thereby decreasing the frequency of spontaneous EPSCs.

## Summary and conclusions

The present study is the first to characterize in detail the spatio-temporal pattern of expression and functional properties of neuronal MHCII molecules in the brain of a non-human primate, the marmoset monkey (*Callithrix jacchus*).

Previous studies in the rodent and feline visual system implicated MHCII in removal of excess synapses in the development of the lateral geniculate nucleus. Surprisingly, in the present study transcripts of MHCII genes in the LGN of both young and adult common marmoset monkeys were not detected; however, these genes were strongly expressed in the primary visual cortex. In young animals (up to the age of one month), *in situ* hybridization revealed that strong MHCII gene expression concentrated mainly in layer IV of the visual cortex, which is the main recipient layer of visual projections from the thalamus, while the expression of these genes appeared more diffuse in older animals. MHCII proteins are expressed strongly in neurons of the primary visual cortex and their temporal pattern of expression follows the main stages of V1 synaptogenesis. To elucidate further the possible involvement of MHCII genes in synaptogenesis, their expression patterns in monocularly enucleated marmosets was analyzed. Our data confirm that MHCII molecules are regulated by neuronal activity. Their specific, patchy distribution in the visual area V1, with high expression levels associated with neurons that receive input from the intact eye, suggests that MHCII molecules may be involved in synaptogenesis.

Furthermore, the distribution and properties of MHCII in the hippocampus of the marmoset monkeys were also investigated. Previous reports on MHCII in hippocampus described them as postsynaptic in rodent hippocampus and implicated them in induction and maintenance of long term depression (LTD). Moreover, MHCII deficient mice display increased frequency

of neurotransmitter release from the synapse. A subset of MHCI molecules that is localized exclusively on the presynaptic side of the mossy fibers-CA3 synapses in the marmoset hippocampus is described here. This subset of MHCI is exclusively localized to giant mossy fiber terminals in the hippocampus. In addition, the properties of excitatory synaptic transmission in acute hippocampal slices of the marmoset monkey were also investigated and it was found that application of antibodies against MHCI interferes with synaptic transmission. Blocking cell-surface MHCI with antibodies resulted in significantly decreased frequency of neurotransmitter release at mossy fiber-CA3 synapses.

These results not only confirm the important role of neuronal MHCI molecules in proper functioning of synapses, but also point to interesting interspecies differences in their distribution, although additional functional analyses are required to assess the significance of these differences.

## References

- Abramoff MD, Magelhaes, P.J., Ram, S.J. (2004) Image processing with ImageJ. *Biophotonics International* 11:36-42.
- Abumaria N, Ribic A, Anacker C, Fuchs E, Flugge G (2008) Stress upregulates TPH1 but not TPH2 mRNA in the rat dorsal raphe nucleus: identification of two TPH2 mRNA splice variants. *Cell Mol Neurobiol* 28:331-342.
- Arosa FA, Santos SG, Powis SJ (2007) Open conformers: the hidden face of MHC-I molecules. *Trends Immunol* 28: 115-123.
- Bellocchio EE, Reimer RJ, Fremeau RT, Jr, Edwards RH (2000) Uptake of glutamate into synaptic vesicles by an inorganic phosphate transporter. *Science* 289: 957-960.
- Berardi N, Pizzorusso T, Ratto GM, Maffei L (2003) Molecular basis of plasticity in the visual cortex. *Trends Neurosci* 26:369-378.
- Biederer T, Sara Y, Mozhayeva M, Atasoy D, Liu X, Kavalali ET, Sudhof TC (2002) SynCAM, a synaptic adhesion molecule that drives synapse assembly. *Science* 297:1525-1531.
- Bourgeois JP, Rakic P (1993) Changes of synaptic density in the primary visual cortex of the macaque monkey from fetal to adult stage. *J Neurosci* 13:2801-2820.
- Bufler J, Kahlert S, Tzartos S, Toyka KV, Maelicke A, Franke C.(1996) Activation and blockade of mouse muscle nicotinic channels by antibodies directed against the binding site of the acetylcholine receptor. *J. Physiol* 492 ( Pt 1): 107-114.
- Cadavid LF, Shufflebotham C, Ruiz FJ, Yeager M, Hughes AL, Watkins DI (1997) Evolutionary instability of the major histocompatibility complex class I loci in New World primates. *Proc Natl Acad Sci USA* 94:14536-14541.

Campbell K, Gotz M (2002) Radial glia: multi-purpose cells for vertebrate brain development. *Trends Neurosci* 25: 235-238.

Cases-Langhoff C, Voss B, Garner AM, Appeltauer U, Takei K, Kindler S, Veh RW, de Camilli P, Gundelfinger ED, Garner CC (1996) Piccolo, a novel 420 kDa protein associated with the presynaptic cytomatrix. *Eur J Cell Biol* 69: 214-223.

Catalano SM, Chang CK, Shatz CJ (1997) Activity-dependent regulation of NMDAR1 immunoreactivity in the developing visual cortex. *J Neurosci* 17:8376-8390.

Corriveau RA, Huh GS, Shatz CJ (1998) Regulation of class I MHC gene expression in the developing and mature CNS by neural activity. *Neuron* 21: 505-520.

Cresswell P, Ackerman AL, Giodini A, Peaper DR, Wearsch PA (2005) Mechanisms of MHC class I-restricted antigen processing and cross-presentation. *Immunol Rev* 207:145-157.

DeBruyn EJ, Casagrande VA (1981) Demonstration of ocular dominance columns in a New World primate by means of monocular deprivation. *Brain Res* 207:453-458.

DeFranco AL, Locksley RM, Robertson M (2007) Immunity: The Immune Response in Infectious and Inflammatory Disease. Oxford University Press.

Fehlmann M, Peyron JF, Samson M, Van Obberghen E, Brandenburg D, Brossette N (1985) Molecular association between major histocompatibility complex class I antigens and insulin receptors in mouse liver membranes. *Proc Natl Acad Sci USA* 82:8634-8637.

Fishman D, Elhyany S, Segal S (2004) Non-immune functions of MHC class I glycoproteins in normal and malignant cells. *Folia Biol (Praha)* 50:35-42.

Fonta C, Chappert C, Imbert M (1997) N-methyl-D-aspartate subunit R1 involvement in the postnatal organization of the primary visual cortex of *Callithrix jacchus*. *J Comp Neurol* 386:260-276.

Fonta C, Chappert C, Imbert M (2000) Effect of monocular deprivation on NMDAR1 immunostaining in ocular dominance columns of the marmoset *Callithrix jacchus*. *Vis Neurosci* 17:345-352.

Fortier MH, Caron E, Hardy MP, Voisin G, Lemieux S, Perreault C, Thibault P (2008) The MHC class I peptide repertoire is molded by the transcriptome. *J Exp Med* 205: 595-610.

Gingras J, Cabana T (1999) Synaptogenesis in the brachial and lumbosacral enlargements of the spinal cord in the postnatal opossum, *Monodelphis domestica*. *J Comp Neurol* 414:551-560.

Goddard CA, Butts DA, Shatz CJ (2007) Regulation of CNS synapses by neuronal MHC class I. *Pro. Natl Acad Sci USA* 104: 6828-6833.

Günther E, Walter L (2001) The major histocompatibility complex of the rat (*Rattus norvegicus*). *Immunogenetics* 53: 520-542.

Hubel DH, Wiesel TN, LeVay S (1977) Plasticity of ocular dominance columns in monkey striate cortex. *Philos Trans R Soc Lond B Biol Sci* 278:377-409.

Henze DA, Urban NN, Barrionuevo G (2000) The multifarious hippocampal mossy fiber pathway: a review. *Neuroscience* 98, 407-427.

Herzog E, Takamori S, Jahn R, Brose N, Wojcik SM (2006) Synaptic and vesicular co-localization of the glutamate transporters VGLUT1 and VGLUT2 in the mouse hippocampus. *J. Neurochem.* 99: 1011-1018.

Hong S, Van Kaer L (1999) Immune privilege: keeping an eye on natural killer T cells. *J Exp Med* 190: 1197-1200.

Huh GS, Boulanger LM, Du H, Riquelme PA, Brotz TM, Shatz CJ (2000) Functional requirement for class I MHC in CNS development and plasticity. *Science* 29: 2155-2159.

Ioannidu S, Walter L, Dressel R, Günther E (2001) Physical map and expression profile of genes of the telomeric class I gene region of the rat MHC. *J Immunol* 166: 3957-3965.

Jindra PT, Jin YP, Jacamo R, Rozengurt E, Reed EF (2008) MHC class I and integrin ligation induce ERK activation via an mTORC2-dependent pathway. *Biochem Biophys Res Commun* 369:781-787.

Jindra PT, Jin YP, Rozengurt E, Reed EF (2008) HLA class I antibody-mediated endothelial cell proliferation via the mTOR pathway. *J Immunol* 180: 2357-2366.

Kaufman J, Salomonsen J, Flajnik M (1994) Evolutionary conservation of MHC class I and class II molecules--different yet the same. *Semin Immunol* 6: 411-424.

Kelley J, Walter L, Trowsdale J (2005) Comparative genomics of major histocompatibility complexes. *Immunogenetics* 56:683-695.

Kirsch J, Betz H (1993) Widespread expression of gephyrin, a putative glycine receptor-tubulin linker protein, in rat brain. *Brain Res* 621: 301-310.

Kulski JK, Shiina T, Anzai T, Kohara S, Inoko H (2002) Comparative genomic analysis of the MHC: the evolution of class I duplication blocks, diversity and complexity from shark to man. *Immunol Rev* 190: 95-122.

Kumanovics A, Takada T, Lindahl KF (2003) Genomic organization of the mammalian MHC. *Annu Rev Immunol* 21:629-657.

Lachance PE, Chaudhuri A (2004) Microarray analysis of developmental plasticity in monkey primary visual cortex. *J Neurochem* 88: 1455-1469.

Laemmli, UK (1970) Cleavage of structural proteins during the assembly of the head of bacteriophage T4. *Nature* 227: 680-685

Lazzari M, Franceschini V (2001) Glial fibrillary acidic protein and vimentin immunoreactivity of astroglial cells in the central nervous system of adult *Podarcis sicula* (Squamata, Lacertidae). *J Anat* 198: 67-75.

Li Q, Lau A, Morris TJ, Guo L, Fordyce CB, Stanley EF (2004) A syntaxin 1, Galpha(o), and N-type calcium channel complex at a presynaptic nerve terminal: analysis by quantitative immunocolocalization. *J Neurosci* 24: 4070-4081.

Lyckman AW, Horng S, Leamey CA, Tropea D, Watakabe A, Van Wart A, McCurry C, Yamamori T, Sur M (2008) Gene expression patterns in visual cortex during the critical period: synaptic stabilization and reversal by visual deprivation. *Proc Natl Acad Sci USA* 105:9409-9414.

Mameli M, Carta M, Partridge LD, Valenzuela CF (2005) Neurosteroid-induced plasticity of immature synapses via retrograde modulation of presynaptic NMDA receptors. *J Neurosci* 25: 2285-2294.

Martin-Pena A, Acebes A, Rodriguez JR, Sorribes A, de Polavieja GG, Fernandez-Funez P, Ferrus A (2006) Age-independent synaptogenesis by phosphoinositide 3 kinase. *J Neurosci* 26: 10199-10208.

McConnell MJ, Huang YH, Datwani A, Shatz CJ (2009) H2-Kb and H2-Db regulate cerebellar long-term depression and limit motor learning. *Proc Natl Acad Sci USA* 106: 6784-6789.

Missler M, Eins S, Merker HJ, Rothe H, Wolff JR (1993) Pre- and postnatal development of the primary visual cortex of the common marmoset. I. A changing space for synaptogenesis. *J Comp Neurol* 333:41-52.

Missler M, Eins S, Merker HJ, Rothe H, Wolff JR (1993) Pre- and postnatal development of the primary visual cortex of the common marmoset. I. A changing space for synaptogenesis. *J Comp Neurol* 333: 41-52.

Missler M, Wolff JR, Rothe H, Heger W, Merker HJ, Treiber A, Scheid R, Crook GA (1992) Developmental biology of the common marmoset: proposal for a "postnatal staging". *J Med Primatol* 21: 285-298.

Neumann H, Cavalie A, Jenne DE, Wekerle H (1995), Induction of MHC class I genes in neurons. *Science* 269:549-552.

Müller BM, Kistner U, Kindler S, Chung WJ, Kuhlendahl S, Fenster SD, Lau LF, Veh RW, Huganir RL, Gundelfinger ED, Garner CC (1996) SAP102, a novel postsynaptic protein that interacts with NMDA receptor complexes in vivo. *Neuron* 17: 255-265.

Neumann H., Cavalie A., Jenne D.E., and Wekerle H. (1995) Induction of MHC class I genes in neurons. *Science* 269, 549-552.

Nicoll RA, Schmitz D (2005) Synaptic plasticity at hippocampal mossy fibre synapses. *Nat Rev Neurosci* 6: 863-876.

Osen-Sand A, Catsicas M, Staple JK, Jones KA, Ayala G, Knowles J, Grenningloh G, Catsicas S (1993) Inhibition of axonal growth by SNAP-25 antisense oligonucleotides in vitro and in vivo. *Nature* 364:445-448.

Oyler GA, Polli JW, Wilson MC, Billingsley ML (1991) Developmental expression of the 25-kDa synaptosomal-associated protein (SNAP-25) in rat brain. *Proc Natl Acad Sci USA* 88:5247-5251.

Phillips ML, Moule ML, Delovitch TL, Yip CC (1986) Class I histocompatibility antigens and insulin receptors: evidence for interactions. *Proc Natl Acad Sci USA* 83:3474-3478.

Rakic P (1976) Prenatal genesis of connections subserving ocular dominance in the rhesus monkey. *Nature* 261:467-471.

Rakic P (1977) Prenatal development of the visual system in rhesus monkey. *Philos Trans R Soc Lond B Biol Sci* 278:245-260.

Ramalingam TS, Chakrabarti A, Edidin M (1997) Interaction of class I human leukocyte antigen (HLA-I) molecules with insulin receptors and its effect on the insulin-signaling cascade. *Mol Biol Cell* 8: 2463-2474.

Reed EF (2003) Signal transduction via MHC class I molecules in endothelial and smooth muscle cells. *Crit Rev Immunol* 23:109-128.

Ririe KM, Rasmussen RP, Wittwer CT (1997) Product differentiation by analysis of DNA melting curves during the polymerase chain reaction. *Anal Biochem* 245:154-160.

Rölleke U, Flügge G, Plehm S, Schlumbohm C, Armstrong VW, Dressel R, Uchanska-Ziegler B, Ziegler A, Fuchs E, Czeh B, Walter L (2006) Differential expression of major histocompatibility complex class I molecules in the brain of a New World monkey, the common marmoset (*Callithrix jacchus*). *J Neuroimmunol* 176:39-50.

Roos C, Walter L (2005) Considerable haplotypic diversity in the RT1-CE class I gene region of the rat major histocompatibility complex. *Immunogenetics* 56: 773-777.

Rozen S, Skaletsky H (2000) Primer3 on the WWW for general users and for biologist programmers. *Methods Mol Biol* 132:365-386.

Saghatelian AK, Gorissen S, Albert M, Hertlein B, Schachner M, Dityatev A (2000) The extracellular matrix molecule tenascin-R and its HNK-1 carbohydrate modulate perisomatic inhibition and long-term potentiation in the CA1 region of the hippocampus. *Eur J Neurosci* 12: 3331-3342.

Sara Y, Biederer T, Atasoy D, Chubykin A, Mozhayeva MG, Sudhof TC, Kavalali ET (2005) Selective capability of SynCAM and neuroligin for functional synapse assembly. *J Neurosci* 25:260-270.

Schebitz H, Brass, W (2007) Operationen an Hund und Katze. Stuttgart: MVS Medizinverlage.

Seress L (2007) Comparative anatomy of the hippocampal dentate gyrus in adult and developing rodents, non-human primates and humans. *Prog Brain Res* 163: 23-41.

Shatz CJ (1996) Emergence of order in visual system development. *Proc Natl Acad Sci USA* 93:602-608.

Shatz CJ, Stryker MP (1978) Ocular dominance in layer IV of the cat's visual cortex and the effects of monocular deprivation. *J Physiol* 281:267-283.

Soares JG, Pereira AC, Botelho EP, Pereira SS, Fiorani M, Gattass R (2005) Differential expression of Zif268 and c-Fos in the primary visual cortex and lateral geniculate nucleus of normal Cebus monkeys and after monocular lesions. *J Comp Neurol* 482: 166-175.

Solheim J.C. (1999) Class I MHC molecules: assembly and antigen presentation. *Immunol Rev* 172: 11-19.

Spatz WB, Illing RB, Weisenhorn DM (1994) Distribution of cytochrome oxidase and parvalbumin in the primary visual cortex of the adult and neonate monkey, *Callithrix jacchus*. *J Comp Neurol* 339:519-534.

Stagsted J, Reaven GM, Hansen T, Goldstein A, Olsson L (1990) Regulation of insulin receptor functions by a peptide derived from a major histocompatibility complex class I antigen. *Cell* 62:297-307.

Stam NJ, Vroom TM, Peters PJ, Pastoors EB, Ploegh HL (1990) HLA-A- and HLA-B-specific monoclonal antibodies reactive with free heavy chains in western blots, in formalin-fixed, paraffin-embedded tissue sections and in cryo-immuno-electron microscopy. *Int Immunol* 2: 113-125.

Sur M, Rubenstein JL (2005) Patterning and plasticity of the cerebral cortex. *Science* 310:805-810.

Tropea D, Kreiman G, Lyckman A, Mukherjee S, Yu H, Horng S, Sur M (2006) Gene expression changes and molecular pathways mediating activity-dependent plasticity in visual cortex. *Nat Neurosci* 9:660-668.

Van der GE, Hof PR, Van Brussel L, Burnat K, Arckens L (2007) Neurofilament protein and neuronal activity markers define regional architectonic parcellation in the mouse visual cortex. *Cereb. Cortex* 17: 2805-2819.

Wong-Riley M (1979) Changes in the visual system of monocularly sutured or enucleated cats demonstrable with cytochrome oxidase histochemistry. *Brain Res* 171:11-28.

Woo J, Cornejo MC, Gao L, Taurog JD, Hammer RE, Buelow R (1997) Monoclonal antibody to the HLA class I alpha 3 domain inhibits T cell activation and prolongs cardiac allograft survival in HLA-transgenic mice. *Transpl Immunol* 5:112-121.

## Curriculum Vitae

**Name:** Adema Ribic

**Date and place of birth:** 15.02.1983. Jajce, Bosnia and Herzegovina

**Nationality:** Bosnian

### Education

- 10/2006-10/2009 PhD Thesis Project at the German Primate Center, Thesis supervisors: PD Dr. Lutz Walter and Prof. Dr. Eberhard Fuchs
- 10/2006-08/2009 Neuroscience Early Stage Research Training (NEUREST)
- 10/2005-10/2009 International MSc/PhD Max Planck Research School in Molecular Biology, Goettingen, Germany
- 10/2000-09/2005 Diploma (General Biology), Faculty of Sciences, University of Sarajevo, Bosnia and Herzegovina

### Scientific courses and workshops

“Physiological characterization of ventricular ciliar cells of mice and their responses to neuropeptides”, 3-10 August 2009, NEUREST Advanced Methods Course, IPMC Sophie-Antipolis, France

“MHC class I on the interface between biology and medicine”, 4-6 July 2008, EMBO/EMBL Workshop, Porto, Portugal

“Introduction to NMR spectroscopy”, 19-21 November 2007, Department of NMR-based Structural Biology, Max Planck Institute for Biophysical Chemistry, Goettingen, Germany

“NMR spectroscopy”, 19-21 November 2007, Department of NMR-based Structural Biology, Max Planck Institute for Biophysical Chemistry, Goettingen, Germany

“Patch-clamp measurements of synaptic transmission in cultured hippocampal neurons”, 21-22 June 2007, Department of Membrane Biophysics, Max Planck Institute for Biophysical Chemistry, Goettingen, Germany

“Molecular biology in yeast applications of the *Tandem Affinity Purification*”, 4-7 June 2007, Department of Neurobiology, Max Planck Institute for Biophysical Chemistry, Goettingen, Germany